1 **A new habitat map of the Lena Delta in Arctic Siberia**

2 **based on field and remote sensing datasets**

3 Simeon Lisovski[1,*], Alexandra Runge[2,*], Iuliia Shevtsova[1], Nele Landgraf[3], Anne Morgenstern[2],

4 Ronald Reagan Okoth[1,4], Matthias Fuchs[2], Nikolay Lashchinskiy[5,6], Carl Stadie[2,7], Alison

5 Beamish[8], Ulrike Herzschuh[1,9,10], Guido Grosse[1,11], Birgit Heim[1]

6

7 [*] Both authors contributed equally

8 [1] Alfred Wegener Institute Helmholtz Centre for Polar and Marine Research, Polar Terrestrial
9 Environmental Systems, 14473 Potsdam, Germany

10 [2] Alfred Wegener Institute Helmholtz Centre for Polar and Marine Research, Permafrost Research, 14473
11 Potsdam, Germany

12 [3] Humboldt University, Department of Geosciences, 12489 Berlin, Germany

13 [4] Julius-Maximilians Universität Würzburg, Institute of Geography and Geology, Oswald-Külpe-Weg 86,
14 97074 Würzburg, Germany

15 [5] Central Siberian Botanical Garden, Siberian Branch, Russian Academy of Sciences, Novosibirsk,
16 630090 Russia

17 [6] Trofimuk Institute of Petroleum Geology and Geophysics, Siberian Branch, Russian Academy of
18 Sciences, Novosibirsk, 630090 Russia

19 [7] University of Greifswald, Institute for Geography and Geology, Germany (current address: University of
20 Copenhagen, Department of Earth Science and Nature Management, Denmark)

21 [8] GFZ German Research Centre for Geosciences, Helmholtz Centre Potsdam.

22 [9] University of Potsdam, Institute of Environmental Sciences & Geography, Karl-Liebknecht-Str. 24-25,
23 14476 Potsdam, Germany

24 [10] University of Potsdam, Institute of Biochemistry and Biology, Karl-Liebknecht-Str. 24-25, 14476
25 Potsdam, Germany

26 [11] University of Potsdam, Institute of Geosciences, Karl-Liebknecht-Str. 24-25, 14476 Potsdam, Germany

27 *Correspondence to*: Simeon Lisovski (Simeon.Lisovski@awi.de), Alexandra Runge
28 (alexandra.runge@gfz-potsdam.de), Birgit Heim (birgit.heim@awi.de)

29

1

Abstract. The Lena Delta is the largest river delta in the Arctic (about 30 000 km2) and prone to rapid changes due to climate warming, associated cryosphere loss and ecological shifts. The delta is characterized by ice-rich permafrost landscapes and consists of geologically and geomorphologically diverse terraces covered with tundra vegetation and of active floodplains, featuring approximately 6 500 km of channels and over 30 000 lakes. Because of its broad landscape and habitat diversity the delta is a biodiversity hotspot with high numbers of nesting and breeding migratory birds, fish, caribou and other mammals and was designated a State Nature Reserve in 1995. Characterizing plant composition, above ground biomass and application of field spectroscopy was a major focus of a 2018 expedition to the delta. These field data collections were linked to Sentinel-2 satellite data to upscale local patterns in land cover and associated habitats to the entire delta. Here, we describe multiple field datasets collected in the Lena Delta during summer 2018 including foliage projective cover (Shevtsova et al., 2021a), above ground biomass (Shevtsova et al., 2021b), and hyperspectral field measurements (Runge et al., 2022, https://doi.pangaea.de/10.1594/PANGAEA.945982). We further describe a detailed Sentinel-2 satellite image-based classification of habitats for the central Lena Delta (Landgraf et al., 2022), an upscaled classification for the entire Lena Delta (Lisovski et al., 2022), as well as a synthesis product for disturbance regimes (Heim and Lisovski, 2023, https://doi.org/10.5281/zenodo.7575691) in the delta that is based on the classification, the described datasets, and field expertise. We present context and detailed methods of these openly available datasets and show how their combined use can improve our understanding of the rapidly changing Arctic tundra system. The new Lena Delta habitat classification represents a first baseline against which future observations can be compared. The link between such detailed habitat classifications and disturbance regime may provide a better understanding of how Arctic lowland landscapes will respond to climate change and how this will impact land surface processes.

2

54 1 Introduction

55 Global warming has profound impacts on the polar regions (Serreze and Barry, 2011; Overland et
56 al., 2019). Rapidly increasing temperatures and changing precipitation regimes result in declining
57 sea ice, warming and thawing of permafrost, more frequent tundra fires, and changes in vegetation
58 (e.g., Biskaborn et al., 2019; Hu et al., 2015; Mauclet et al., 2022; Box et al., 2019; Amap, 2021).
59 The Arctic tundra biome, which is normally characterized by harsh living conditions and nutrient-
60 deficiency, has experienced rapid phenological shifts, such as earlier green-up in spring, which is
61 also associated with increasing shrubification rates (Mekonnen et al., 2021). Shifts in plant
62 communities are also driven by changing nutrient availability in permafrost soils (Mekonnen et al.,
63 2021; Mauclet et al., 2022), affecting the net primary productivity of tundra ecosystems.

64 Satellite-derived remote sensing can provide large-scale assessments of Arctic vegetation cover and
65 changes therein (Bartsch et al., 2016). For example, the Circumpolar Arctic Vegetation Map (CAVM)
66 project, from the Conservation of Arctic Flora and Fauna working group (CAFF), provided a first
67 panarctic vegetation composition map based on Advanced Very-High Resolution Radiometer
68 (AVHRR) false-color infrared (CIR) composites at a 1:4 million map scale (Walker, 1998; Raynolds
69 et al., 2019). Later, higher resolution land cover maps became available across all spatial scales
70 from national and international efforts such as the NASA Arctic-Boreal Vulnerability Experiment
71 (ABoVE) providing open-source data collections from boreal and arctic regions (ABoVE Science
72 Definition Team, 2014) specifically for Alaska, Canada, Northern Europe, and Western Siberia,
73 providing a better bridge to field measurements. Such products greatly assist in monitoring and
74 upscaling of patterns and dynamics of soil properties, land-atmosphere fluxes, ecosystem states,
75 and changes therein (e.g., Walker, 1998; Beamish et al., 2020; Berner et al., 2020; Sweeney et al.,
76 2022; Macander et al., 2022; Endsley et al., 2022). For selected Eastern Siberian tundra regions,
77 land cover maps have been produced (e.g., Veremeeva and Gubin, 2009; Bartsch et al., 2019;
78 Schneider et al., 2009), including the Lena Delta (Bartsch et al., 2019; Schneider et al., 2009).

79 Arctic river deltas represent distinct and vulnerable geomorphological and ecological regions at the
80 marine-terrestrial boundary. River deltas have been studied intensively to better understand land
81 cover and vegetation compositions (Jorgenson, 2000; Schneider et al., 2009; Frost et al., 2020;
82 Bartsch et al., 2020), carbon pools and fluxes (Bartlett et al., 1992; Schneider et al., 2009; Sachs et
83 al., 2008; Rossger et al., 2022), and land cover change caused by climate change impacts
84 (Jorgenson, 2000; Pisaric et al., 2011; Lantz et al., 2015; Nitze and Grosse, 2016; Vulis et al., 2021;
85 Juhls et al., 2021). With diverse habitats, Arctic river deltas are biodiversity hotspots (Gilg et al.,
86 2000), but at the same time are prone to rapid changes (Walker, 1998; Overeem et al., 2022). Arctic

3

87　deltas are affected by permafrost thaw (e.g., Pisaric et al., 2011; Nitze and Grosse, 2016; Vulis et

88　al., 2021), sea ice loss (Overeem et al., 2022), and increased sediment transport and organic load

89　during spring floods (Piliouras and Rowland, 2020; Juhls et al., 2021). Arctic river deltas are very

90　dynamic systems and high-resolution habitat information from these biodiversity hotspots is needed

91　to assess and predict changes and implications of Arctic warming.

92　The Lena Delta is the largest Arctic river delta representing a typical lake-rich lowland permafrost

93　landscape (Grigoriev, 1993). Over the past decades, the central Lena Delta became a place of

94　intensive international research. In addition to long-term permafrost monitoring at the Research

95　Station Samoylov Island (Hubberten et al., 2006; Boike et al., 2019), extensive records on

96　meteorology, soil and ecosystem characteristics (Zibulski et al., 2016; Boike et al., 2019; Boike et al.,

97　2008), hydrology (Fedorova et al., 2015), and greenhouse gas fluxes (Rossger et al., 2022; Holl et

98　al., 2019) are available, setting an important benchmark for further assessments of changes in an

99　Arctic river delta. During the summer season of 2018, an extensive field campaign to the Lena Delta

100　led to an unprecedented amount of field datasets including vegetation cover recordings, above

101　ground biomass estimates, and spectral characterisation of the different vegetation/land cover units.

102　These in situ datasets provide improved thematic detail allowing the development of habitat

103　classifications. In 2009, Schneider et al. (2009) developed the first land cover classification map for

104　the entire delta at 30 m spatial resolution based on Landsat-7 ETM+ satellite summer images from

105　2000 and 2001 to quantify delta-wide methane emissions. The availability of Sentinel-2 (S-2)

106　Multispectral Instrument (MSI) data from two orbiting satellite missions since 2016 and 2017 provide

107　high quality multispectral satellite data with a higher spatial resolution in the Visible and Near

108　Infrared wavelength of up to 10 m, and of 20 m in the Red Edge and the Short- Wave Infrared

109　wavelength regions (Drusch et al., 2012, ESA 2015). Together with the extensive ground

110　observations from the Lena Delta in 2018 this enables an updated classification, using the higher

111　resolution S-2 images and improved thematic detail.

112　In the following study, field datasets as well as derived multispectral satellite images from the

113　summer season 2018 for the Lena Delta were used to provide 1) an updated data-driven framework

114　for plant communities and associated habitat classes in the Lena Delta, 2) a high-resolution habitat

115　mapping product for the entire delta, and 3) a disturbance regime map linked to habitat classes.

116　These datasets enhance our understanding of the Lena Delta system and will build a baseline and

117　framework for future spatio-temporal analysis of more detailed processes and changes within this

118　highly sensitive ecosystem.

4

2 Study Area

The Lena Delta is located in northeastern Siberia's continuous permafrost zone between 72° and 74°N and 123° to 130°E (Figure 1). With an area of about 30 000 km^2, it is the largest delta in the Arctic and one of the largest in the world (Walker, 1998; Schneider et al., 2009). It is surrounded by the Laptev Sea to the west, north, and east, and the Chekanovsky and Kharaulakh mountain ranges border it to the south. The delta is characterized by numerous river channels and more than 1500 islands with a diverse geologic history (Grigoriev, 1993). Morphologically, the delta can be divided into three distinct geomorphological main terraces (Grigoriev, 1993; Schwamborn et al., 2002). The first main terrace, which comprises the Holocene fluvial terraces and the active floodplains, is the youngest and most active part of the delta (Schwamborn et al., 2023), and covers most of the east-northeastern areas as well as the southern and southwestern-most parts This main terrace predominantly consists of ice wedge-polygonal tundra (Nitzbon et al., 2020) as well as of barren and vegetated floodplain areas (e.g., Rossger et al., 2022). The second main terrace, located in the northwestern part, contains mostly sandy, comparably well-drained soils with low ground-ice content (Schwamborn et al., 2002; Ulrich et al., 2009). Large, mostly north-to-south oriented lakes and depressions are abundant in this area (Morgenstern et al., 2008). The third and oldest main terrace consists mainly of remnants of a Late Pleistocene accumulation plain with ice- and organic-rich sediments (so-called Yedoma deposits) and is characterized by polygonal tundra with large ice wedges, deep thermokarst lake basins, and thermo-erosional valleys (Morgenstern et al., 2011; Morgenstern et al., 2021). The third terrace is found on islands in the southern delta region (Schirrmeister et al., 2003; Schirrmeister et al., 2011). Permafrost in the area has a thickness of about 500–600 m (Romanovskii and Hubberten, 2001). The active layer depth, i.e., the seasonally thawing upper soil layer, on the first terrace is usually in the range of 30 to 50 cm and 80 to 120 cm on the floodplains (Boike et al., 2019). The larger region is characterized by an Arctic continental climate with low mean annual air temperatures of −13 °C, a mean temperature in January of −32 °C, and a mean temperature in July of 6.5 °C. The mean annual precipitation is low and amounts to about 190 mm (World Weather Information Service).

As part of past Russian-German expeditions to the Lena Delta, most research during the last two decades has been carried out on the islands of Samoylov and Kurungnakh in the central delta (Figure 1). Samoylov Island (72°22′ N, 126°29′ E) covers an area of about 5 km^2 and is representative of the first terrace together with an active floodplain (Boike et al., 2019; Boike et al., 2008). The vegetation and soil types are diverse at local scales due to high lateral variability of the polygonal microrelief consisting of drier polygon rims, and moist to wet polygonal depressions and troughs (Nitzbon et al., 2020; Kienast and Tsherkasova, 2001). In contrast, Kurungnakh Island is

5

153 mainly composed of late Pleistocene Yedoma deposits that belong to the third delta terrace

154 (Grigoriev, 1993) with elevation up to 55 m above sea level (m a.s.l.) (Morgenstern et al., 2013).

155 Holocene cover deposits and peat-rich permafrost soils are distributed across the surface of the third

156 Lena River terrace and especially concentrated in the deep thermokarst basins called "alases".

157 Alases are important landscape-forming features of the ice-rich Yedoma permafrost zone, which are

158 mainly caused by extensive melting of excess ground ice in the underlying permafrost (Van

159 Everdingen, 1998).

160

161 3 Datasets and methods

162 Several new datasets are presented for the Lena Delta that are spatially and thematically connected

163 and support vegetation, habitat, and land cover applications for this region (Figure 1).

164 Two datasets feature field-measured vegetation data, providing information on foliage projective

165 cover (Dataset 1) and above ground biomass (Dataset 2) recorded in the central Lena Delta in

166 summer 2018 across 26 selected vegetation plot sites (supplementary table S1, S2). The field plots

167 of 30 x 30 m (900 m^2) were chosen to be representative for typical vegetation communities (vascular

168 plants, moss and lichen cover) as largely homogenous sites representative for the surrounding area.

169 In addition, a total of 28 in-situ, canopy-level hyperspectral field measurements were acquired in 30

170 x 30 m plots with homogeneous vegetation or barren to partially vegetated areas (spectral

171 reflectance field measurements; Dataset 3). Of the 28 hyperspectral measurements, 15 were

172 conducted at the vegetation plot sites of Datasets 1,2 three measurements were repeat

173 measurements to capture vegetation senescence, and at 10 spectrometry plots we conducted

174 hyperspectral field measurements without floristic inventories but with detailed plot documentation.

175 Based on expert knowledge, we defined representative habitat classes and identified homogeneous

176 regions within the central Lena Delta to train and apply a classifier using a S-2 satellite image from

177 summer 2018 (Dataset 4). Due to the high reliability of the central Lena Delta vegetation

178 classification and positive evaluation by field experts, we used this vegetation classification as a

179 training dataset for a robust classifier that was subsequently applied to a S-2 image mosaic for the

180 entire Lena Delta for 2018 to develop a new Lena Delta habitat map (Dataset 5).

181 Finally, using the habitat classes, probability maps for exposed sandbars and water distribution, and

182 information from the in-situ dataset (Datasets 1 & 2), we extrapolated a classification of disturbance

183 regimes across the delta (Dataset 6) as an application example for the habitat classes.

6

3.1 Foliage projective cover (Dataset 1)

185 A detailed description of plant composition for the 26 vegetation plots of the 2018 expedition to the
186 Lena Delta was compiled (see supplementary table S1, S2, S3). Prior to the field work, the
187 approximate site locations were defined for establishing representative vegetation plots based on
188 field knowledge and evaluation of Landsat and Sentinel-2 satellite imagery. The aim was to cover
189 representative vegetation communities of the central delta. There are vegetation communities with
190 large area coverage that show high homogeneity within larger areas (10s of meters). Therefore, at
191 each site location, we defined a 30 x 30 m square plot with a homogeneous or repetitive vegetation
192 composition that was also representative of the wider land surface serving as an Elementary
193 Sampling Unit (ESU). ESUs according to the Committee on Earth Observing Satellites Working
194 Group on Calibration and Validation (Duncanson et al., 2021) serve as spatial training and
195 validation units representative for the land surface for quantitative and qualitative remote
196 sensing operations. In case of more patchy and heterogeneous vegetation structure we selected 30
197 x 30 m squares embedded in a minimum of 50 x 50 m square of the same vegetation composition.

198 The detailed floristic composition was recorded around the plot center in four successive rings of 50
199 cm diameter. In addition, the vegetation plot was mapped in detail from above with one Red-Green-
200 Blue (RGB) and one Red-Green-Near Infrared (RGNIR) MAPIR camera using telescope stick-based
201 field photography. The projective vegetation cover was recorded in at least three subplots (2 m x 2
202 m) within the plot. If the vegetation cover was highly homogenous three subplots were established.
203 In the case of moisture differences, e.g. in polygonal tundra with dry rims and moist to wet
204 depressions, we established higher numbers of subplots capturing moist as well as dry patches
205 (see, Figure 2 & 3 describing the concept). We compiled the floristic composition to foliage projective
206 cover by plant taxa on each 2 x 2 m subplot for the different canopy levels and extrapolated for the
207 30 m x 30 m plot. We used the RGB and NIR field photos to make an estimate on the share of moist
208 and dry surface area to calculate an averaged projective vegetation cover. The ring survey data was
209 not included in the plot average. The dataset of percentage foliage projective cover per vegetation
210 plot is published in PANGAEA (Shevtsova et al., 2021a,
211 https://doi.pangaea.de/10.1594/PANGAEA.935875).

3.2 Above ground plant biomass (Dataset 2)

213 Above-ground biomass (ABG) was sampled in the field in 25 of the 26 vegetation plots in 2018 (see
214 supplementary table S1, S2, S3). Within each 2 x 2 m subplot a 0.5 m x 0.5 m representative plot

215 was selected for ABG sampling. AGB sampling for moss and lichens was conducted within 0.1 m x

216 0.1 m subplots inside the 0.5 m x 0.5 m subplots.

217 In total, 174 fresh AGB samples were collected and weighed in the field or subsequently at the

218 Samoylov research station. AGB samples with a weight exceeding 15 g were subsampled. The plant

219 samples were then dried for two to four days in a warm dry place and finally oven-dried for ca. 24

220 hours at a temperature of 60 °C before re-weighing. All AGB assessments per plant community type

221 were upscaled to the 30 m x 30 m plot in g/m^2 using the foliage projective cover data. The dataset of

222 AGB per vegetation plot has been published in PANGAEA (Shevtsova et al., 2021b,

223 https://doi.pangaea.de/10.1594/PANGAEA.935923).

224 **3.3 Hyperspectral field measurements (Dataset 3)**

225 Hyperspectral field measurements were conducted in the central Lena Delta in August 2018 with the

226 aim to collect surface reflectance spectra of different homogeneous land cover units across a variety

227 of delta land surfaces and vegetation composition. In total, we collected 28 hyperspectral field

228 measurements in homogeneous 30 x 30 m spectrometry plots (Table S5), with 15 of them equalling

229 the vegetation plots across Samoylov and Kurungnakh islands (see Dataset 1 & 2 *and*

230 *supplementary table S4),* three as repeat measurements at the end of August to capture the change

231 in spectral signature during senescence since the beginning of August and the remaining 10 field-

232 spectroscopy plots focusing on non-vegetated areas such as sandy parts of the floodplain*.* We

233 conducted the field-spectroscopy measurements with a Spectral Evolution SR-2500 field

234 spectrometer with a 1.5 m Fiber Optic Cable. The instrument was calibrated to spectral radiance

235 within a wavelength range of 350 to 2500 nm. Within the 30 x 30 m homogeneous spectrometry

236 plots we acquired about 100 individual measurements, randomly scattered across the plot. Before

237 and after each survey we conducted reference measurements by measuring the back reflected

238 downwelling radiance from a Zenith Lite[TM] Diffuse Reflectance Target of 50% reflectivity to normalize

239 to surface reflectance percentages per wavelength. The averaged individual measurements of the

240 reflectance of each spectrometry plot was published in the PANGAEA data repository (Runge et al.,

241 2022, https://doi.pangaea.de/10.1594/PANGAEA.945982).

242 **3.4 Central Lena Delta habitat classification (Dataset 4)**

243 *3.4.1 Habitat classes*

244 Based on the vegetation plots (Dataset 1 & 2) and from field knowledge, different habitat classes

245 characterized by distinct plant communities, moisture regimes and soil properties were defined. Non-

246 vegetated areas (e.g., sand) and water were added as additional classes using band thresholds

247 (Table 1). During an iterative process within aS-2 based supervised classification, additional habitat

248 classes that were not covered by the vegetation plots (Dataset 1 & 2) were added: i) The polygonal

249 tundra complex could spectrally be separated into distinct classes related to different surface water

250 abundance in the form of intra- and interpolygonal ponds, therefore, we implemented three different

251 polygonal tundra complex classes, with up to 10%, 20%, 50% surface water cover respectively, and

252 ii) one class of 'sparsely vegetated' representing the areas of transition zones between vegetated

253 and barren. Table 1 provides details on habitat class descriptions and established methods to

254 distinguish habitats.

255 *3.4.2 Satellite data processing*

256 The central Lena Delta habitat classification is based on one high quality cloudless S-2) image from

257 August 6 in 2018, representing the late summer. The S-2 top of atmosphere reflectance (TOA)

258 image data was processed by the German Space Agency DLR (B. Pflug, oral communication, 2019)

259 to bottom of atmosphere (BOA) surface reflectance using the newest version of the atmospheric

260 correction processor Sen2Cor later released as ESA Sen2Cor in 2020. Atmospheric correction

261 processing was performed with the default rural aerosol model. All spectral bands were resampled to

262 the 10 m pixel resolution bands. The 60 m pixel resolution bands (B1, B9, B10) that support

263 atmospheric correction, but are not optimal for land surface classification, were removed. We added

264 the normalized difference vegetation index (NDVI; NIR-RED / NIR + RED) to the band collection.

265 *3.4.3 Central delta habitat classification*

266 S-2 pixels from the 30 x 30 m ESUs (dataset 1, Shevtsova et al. 2021a), and additional polygons

267 defined by expert knowledge, led to 8 626 training pixels (50% to train the classifier and 50% for

268 validation) for the habitat classification (training points shown in Appendix A4 and are published in

269 the Landgraf et al 2022a data collection). We tested several classifiers and different selected band

270 combinations (spectral bands and NDVI). Water (transparent to turbid) and sandbanks were omitted

271 in the classification processing by masking them as inactive using a band threshold; water mask was

272 based on the NIR 10 m band 8 (NIR < 0.02) and the sand mask was based on the blue 10 m band 2

273 (Blue > 0.07, Table 1). The classification was tuned to depict vegetation composition and was

274 qualitatively assessed well known to the classification developers. Best results for the habitat

275 classification were obtained using a random forest classification with a band combination of all S-2

276 VIS, Red-Edge, NIR and SWIR bands, and the NDVI. The chosen classifier was able to distinguish

277 between relevant classes (Table 1) and could even identify patchy spots of specific habitat classes.

278 In addition to the defined water and sand classes, the final central Lena Delta classification contains

9

279   10 habitat classes (Table 1). The here defined central Lena Delta covers an area of 644.9 km^2 with a
280   55.2 % vegetation cover.

281   To assess the classification performance we applied a cross-validation on an independent random
282   selection of the training pixels (50 %). Based on a confusion matrix (supplementary table S5), the
283   classification accuracy was 96.78 %. However, this is partly due to strong autocorrelation resulting
284   from pixel selection within polygons. More importantly, the accuracy was qualitatively tuned and
285   evaluated based on ground-truthed knowledge of the development team. The published dataset of
286   Landgraf et al. (2022, https://doi.pangaea.de/10.1594/PANGAEA.945057) provides the central Lena
287   Delta habitat classification map, the ESUs and the polygons used to train the classifier. The training
288   dataset includes data from 23 of the 26 vegetation plots (dataset 1). The dataset provides additional
289   69 ESUs defined with expert knowledge gathered during several field expeditions to the Lena Delta,
290   labeled as pseudo ESUs for potential future investigations.

291   **3.5 Lena Delta habitat classification (Dataset 5)**

292   *3.5.1 Lena Delta habitat classes*

293   In order to extend the habitat classification map to the entire Lena Delta (29873.7 km^2), we included
294   all the habitat classes covering the central Lena Delta (dataset 4, table 1). In addition, and based on
295   expert knowledge as well as extensive visual satellite image investigations, we added one habitat
296   class that is not present in the central Lena Delta: the second terrace in the northwest of the Lena
297   Delta is lithologically and geomorphologically different from the other two terraces present in the
298   central delta, and characterized by sandy substrates. In a hyperspectral CHRIS PROBA satellite-
299   based geomorphological classification, Ulrich et al. (2009) described the second terrace featuring
300   very dry elevated sandbanks, barren or poorly vegetated areas with isolated lichens, moss, herbs,
301   dwarf shrubs or grasses (vegetation cover 0–60%, growth height: max. 20 cm, average active layer
302   depth of 1 m on the upland plain with old, vegetation-arrested sand dunes). Based on photos taken
303   at few locations in the field during past expeditions (see supplementary table S3) the habitat class
304   shows well-drained areas dominated by sandy substrate and diverse, sparse vegetation cover; some
305   areas are dominated by sedges, cotton grass and mosses with rare occurrences of lichens and
306   dwarf shrubs, while some areas are dominated by the latter. Schneider et al. (2009) defined the
307   same class as 'dry moss-, sedge- and dwarf shrub-dominated tundra (DMSD)'. We selected 35
308   ESUs for this habitat class characterized by high SWIR reflectance (S-2 band 11) due to dry land
309   surface conditions. The habitat class was named 'dwarf shrub - herb communities' and was added
310   as an additional habitat class to the training data set.

311

10

312   *3.5.2 Satellite data processing*

313   The Lena Delta habitat classification was based on a S-2 mosaic (top of atmosphere (TOA)

314   reflectance, Google Earth Engine Dataset) with images taken of the area between June 1 and

315   September 15, 2018. The images (N = 1685, distributed across 15 S-2 tiles) were filtered to discard

316   images with cloud cover above 20%. A cloud mask was applied to the remaining 262 images,

317   masking pixels where the quality band 'QA60' indicates clouds (band 10) or cirrus (band 11). All

318   spectral bands with 20 m resolution were resampled to match the 10 m resolution bands. Next, NDVI

319   was computed (see 3.4) for each image and one high-quality mosaic of all images based on the

320   maximum NDVI value per pixel was produced representing a snapshot of the peak summer

321   vegetation period. Using the median NIR band values across the 262 cloud-masked images, we

322   classified water with a threshold of < 0.07 reflectance. The remaining non-vegetated areas defined

323   by a threshold of NDVI < 0.4 were classified as barren/sand. The water- and sand-masked image

324   mosaics were then used in the classification pipeline with the following bands: B2 (blue), B3 (green),

325   B4 (red), B5 (red edge 1), B6 (red edge 2), B7 (red edge 3), B8 (NIR), B11 (SWIR 1), B12 (SWIR 2),

326   and NDVI.

327   *3.5.3 Lena Delta Habitat classification*

328   From the central Lena Delta habitat classification (dataset 4) we sampled 7 500 random pixels to

329   train a random forest classifier (smileRandomForest in Google Earth Engine). In addition we added

330   35 pixels from the ESUs selected within the 'dwarf shrub - herb communities' of the north-western

331   Lena Delta. Unfortunately, no vegetation recording/monitoring schemes exist outside the central

332   Lena Delta. Therefore, independent validation of the classification across the Delta is not possible.

333   Similar to the validation of the central Lena Delta habitat classification, the results were carefully

334   checked with expert knowledge from the central Delta and a few adjacent regions that are known to

335   the developer team. Together with visual comparison of high resolution ESRI RGB satellite

336   background images, we consider the results accurate. A formal validation based on another random

337   sample of 5 000 points from the central Delta showed expected high accuracy of > 95 %.

338   Since the barren/sandy areas are highly dynamic with variable water levels mainly within (due to

339   flooding in spring and decreasing river flow during the summer season) but also across years

340   (discharge dynamics), we computed a sandbar probability map for the Lena Delta using cloud

341   masked S-2 (TOA reflectance) images between April 1 and October 15 from 2015 to 2021 (6 026

342   images). In each image, we labeled sandy pixels by NDVI < 0.4 AND NDWI > 0.095 AND NIR < 0.09

343   reflectance. Next, for each pixel in the Lena Delta, we computed the percentage of sandy pixels

344   across all images resulting in a sand probability map. The training dataset (random 7500 points, plus

11

345   35 points with label 'dwarf shrubs - herb communities'), the habitat classification, and the sandbar

346   probability map was published in the PANGAEA repository (Figure 5, Lisovski et al., 2022,

347   https://doi.pangaea.de/10.1594/PANGAEA.946407).

348   **3.6 Lena Delta disturbance regimes (Dataset 6)**

349   The Lena Delta experiences different disturbance regimes, mapped and described in dataset 6.

350   Mainly annual flooding, but also local rapid thaw processes on the land surface of the terraces with

351   ice-rich permafrost, result in disturbance regimes forming distinct habitat classes (Table 2). The

352   floodplains experience seasonal flooding as a regularly occurring disturbance in spring after ice-

353   break up (the spring flood). Very high disturbance regimes due to the most intense scour, erosion

354   and sedimentation result in barren sandbanks or in early-stage plant communities equalling the

355   'sparsely vegetated' habitat class. The classes 'moist to wet sedge communities', 'wet sedge

356   communities', 'moist equisetum and shrubs', 'dry shrub communities', 'dry grass to wet sedge

357   communities' represent the mid to advanced successional stages on the floodplain within areas of

358   high disturbance that are also described as shifting habitat class (Stanford et al., 2005; Driscoll and

359   Hauer, 2019).

360   In contrast to the high disturbance regimes on the floodplain, habitats on the first, second and third

361   delta terraces are less extensively disturbed (low disturbance). In these areas typical mature-state

362   tundra plant communities are able to develop; 'polygonal tundra complex', 'tussock tundra', and

363   'dwarsh shrub herb communities'. However, locally, high disturbance occurs by rapid thaw

364   processes of ice-rich permafrost on the first and third delta terraces with habitats characterized by

365   mid to advanced-stage plant succession; 'moist to wet sedge communities', 'wet sedge

366   communities', 'dry shrub communities', and 'dry grass to wet sedge' communities. Very high

367   disturbance due to intense rapid thaw processes occurs at eroding cliffs and lake margins, in steep

368   valleys and actively developing gullies resulting in barren surfaces with rims of sparsely vegetated

369   transition zones. Given the link between plant communities and flooding as well as rapid thaw

370   processes, we characterized the disturbance regimes for each habitat class (Table 2) and provide

371   mapped disturbance based on the habitat class of dataset 5 and the corresponding disturbance

372   regime for the entire Lena Delta (Figure 6, Heim and Lisovski, 2023,

373   https://doi.org/10.5281/zenodo.7575691).

12

374 4 Results and Discussion

375 We deliver a detailed description and associated data products of the most prominent habitat
376 classes in the largest Arctic river delta, the Lena Delta. Supported by ecological field data of plant
377 composition, hyperspectral field measurements from the same sites, and regional expert knowledge
378 collected over decades, we develop a high-resolution S-2 based habitat map for the entire delta. The
379 compiled datasets provide the necessary baseline for future investigations of the biochemical
380 processes, ecological dynamics, and responses to global warming within the Arctic tundra system of
381 the delta.

382 **4.1 Habitat classes of the Lena Delta**

383 Based on the floristic composition and biomass of the vegetation plots (Dataset 1, 2), the spectral
384 properties from hyperspectral field measurements (Dataset 3) as well as expert knowledge, we
385 defined 11 distinct habitat classes linked to different vegetation composition for the Lena Delta
386 (Figure 4). The selected S-2 spectral bands and the derived NDVI values allow a separation of the
387 habitat classes into two distinct groups (the first separation level between habitat classes in Figure
388 4a, 1st hierarchical level). Three habitat classes ('wet sedge communities', 'moist Equisetum and
389 shrub communities', 'dry grass to wet sedge communities') formed in areas of high disturbance by
390 rapid thaw processes and regular flooding represent a distinct cluster with highest vegetation vitality
391 (high NDVI), and separated from the more stable and mature tundra communities ('polygonal tundra
392 complex', 'dry (tussock) tundra', and 'dry dwarf-shrub and herb communities'), and the other
393 successional plant communities ('moist to wet sedge complex', 'dry low shrub communities' and
394 'sparsely vegetated') all characterised by a lower NDVI range. The 'dry dwarf-shrub and herb
395 communities' form a separate cluster with the least overlap with other habitat classes within the two-
396 dimensional non-metric multidimensional scaling (NMDS) space (2nd hierarchical level, Figure 3a;
397 Figure 4c) due to very low vegetation vitality and surface moisture (lowest NDVI, high red and SWIR
398 reflectance). There are two remaining habitat classes on the 3rd and 4th hierarchical level, which are
399 successional plant communities, the 'moist to wet sedge complex' and 'dry low shrub communities'.
400 The separation on the 3rd and 4th hierarchical level is mainly driven by higher NDVI of these
401 successional plant community classes in comparison with the mature state tundra plant communities
402 with lower NDVI (Figure 4a-b). The 'dry grass to wet sedge communities' and the 'sparsely
403 vegetated area' habitat class (not covered by vegetation plots but added during the classification
404 process), show the largest overlap with the other habitat classes due to a high variability in
405 vegetation cover, biomass and moisture. In general, the ordination method (Figure 4b) shows that
406 distinct plant communities and the associated habitat classes are mostly separated by a biomass

407 gradient for which the NDVI is a good approximator. A further separation linked to potential spectral
408 proxies for biomass exists with the far red-edge and NIR bands (B6,7,8) but is less distinct than the
409 NDVI axis. Together with the SWIR (B11,12) the red (B4) and near red-edge (B5) bands, and less
410 strongly the blue and green bands (B2,3), the results indicate a habitat class separation based on
411 moisture, biomass and vegetation colour characteristics.

412 The vegetation plot selection was made in relation to the most typical habitats (e.g., Mueller-
413 Bombois and Ellenberg, 1974). For 15 of the 26 vegetation plots, we collected and provided
414 hyperspectral surface reflectance data (Runge et al., 2021). These measurements cover a variety of
415 landscape units including Yedoma uplands, floodplains (vegetated and non-vegetated), drained
416 thermokarst lake basins (old and recently drained), and areas covered by low shrub layers.
417 Comparing the hyperspectral surface reflectance with multispectral S-2 data, we found
418 commonalities in the discrimination of habitat classes along moisture gradients. Unfortunately, the
419 hyperspectral field measurements do not cover the biomass gradient. Plot measurements with the
420 field spectrometer are conducted with the hand-held instrument held at shoulder height, hence it was
421 not possible to acquire field spectroscopy measurements in disturbed patches with tall shrubs or
422 very sloped terrain. This highlights the difficulty in deriving high spectral resolution surface
423 reflectance measurements representative of fine scale differences between Arctic tundra habitat
424 classes if the plot properties become too challenging to measure.

425 In general, mature-state tundra plant communities have relatively similar spectral properties due to
426 low vascular plant cover (e.g., Beamish et al., 2017). In addition, the tundra vegetation communities
427 contain a wide range of accessory pigment composition (carotenoids and anthocyanins) that result in
428 a very similar spectral response (Beamish et al., 2018). Only the highly disturbed communities such
429 as wetlands or areas with tall shrubs are more spectrally distinct due to a high NIR reflectance
430 plateau (Buchhorn et al., 2013). Since the hyperspectral field measurements provide a higher spatial
431 resolution and thus also a measure of variability within areas of the same general habitat type, we
432 consider the measurements valuable for applications that aim at analysing ecological and
433 biochemical processes within distinct habitats in more detail.

434 **4.2 Sentinel-2 based habitat classification**

435 Based on the identified habitat classes (Table 1) we applied a random forest classifier to map habitat
436 classes in the central Lena Delta and subsequently in the entire Lena Delta. Both maps represent
437 the summer season of 2018 for which we could use a sufficient number of satellite images with low
438 cloud cover.

14

439   The Lena Delta habitat map shows the ice-rich first and third terraces mainly covered by i) the

440   'polygonal tundra complex' due to impeded drainage on the terrace plateaus and by ii) drier tundra

441   communities on well drained areas due to older degraded permafrost forms (detailed description in

442   Morgenstern et al., 2008, 2011). On the second terrace, the classified 'dry dwarf shrub and herb

443   communities' occur well separated from the moist habitat classes covering the floor of the alases.

444   On the floodplains, the rich mosaic outlines a wide spectrum of very diverse classes, the dry versus

445   moist and wet substrate habitats, in the active delta area.

446   Polygonal tundra is characterized by high spatial heterogeneity; at the decimeter to meter-scale

447   plant composition and diversity is defined by the polygonal microrelief and water level (Whitaker and

448   Woodwell, 1968; Forman and Godron, 1981; Zibulski et al., 2016; Nitzbon et al., 2020, Siewert et al.,

449   2021). Therefore, within a single S-2 pixel, dry polygonal rims, moist slopes, wet patches and

450   surface water can all be present. The spatial resolution of S-2 cannot capture the meter-scale, but

451   captures the heterogeneity between the different surface water contributions of the 'polygonal tundra

452   complex' on the first and third terrace. In the Lena Delta, the 'polygonal tundra complex with up to

453   50% surface water' represents the dominant habitat class with 25% of the delta area (about 7 434

454   km^2). All other habitat classes represent 1-6% of the delta area with 'dwarf shrub-herb communities'

455   and 'moist to wet sedge complex' reaching 5.4% and 5.9%, respectively (Figure 6). Based on the

456   summer S-2 mosaic, the classes 'Water' and 'Sand' cover more than 40% of the delta. However,

457   those two classes are extremely variable within and across years, depending on the river water level

458   during image acquisition time. To provide information on this variability, we calculated how often

459   each pixel in the delta (cloud free S-2 pixels from 2015 to 2022) was classified as sand (threshold

460   approach). This led to an additional sand probability layer with values between 0-100%.

461   Despite extensive research within the area, only a few classification products are available for the

462   Lena Delta. The new Lena Delta classification is a high-resolution (S-2, 10 m) map that focuses on

463   the delta-specific habitat classes and emphasizes the high level of heterogeneity across the delta.

464   We compared the Lena Delta habitat classification to existing classifications: the first published Lena

465   Delta-wide land cover classification targeted towards tundra environments and the upscaling of

466   methane emissions with 30 m resolution (Schneider et al., 2009), the global ESA Climate Change

467   Initiative CCI land cover classification with 300 m resolution (Defourny, 2019), and a circum-arctic

468   standardized ESA GlobPermafrost land cover map of the Lena Delta with 20 m resolution (Bartsch

469   et al., 2019). We sampled the classification results with a regular point grid of more than 3 million

470   points which have an equal distance of 100 m to one another to compare the classification results.

471   Figures and tables with more information on class comparisons can be found in the supplements

472   (Table 1, Figure S3, S4m, S5). Overall, the classifications of the Lena Delta overlap well for 'water'

473   (water bodies (Defourny, 2019), shallow water (Schneider et al., 2009), water (different depths and

474   sediment yields, Bartsch et al. 2019)) and 'sand' (bare areas (Defourny, 2019), mainly non-

475   vegetated areas (Schneider et al., 2009), sand, seasonally inundated and disturbed (Bartsch et al.

476   2019)) areas. Besides this, the mapped classes differ greatly from one another. For example, the

477   dominant classes in the coarse ESA CCI land cover 2018 product (300 m) for the Lena Delta are

478   'shrub or herbaceous cover', 'flooded', 'fresh / saline / brackish water', 'sparse vegetation (tree,

479   shrub, herbaceous cover) (<15%)', and 'mosaic tree and shrub (>50%)', 'herbaceous cover (>50%)'.

480   These broad classes describe the major land cover in the Arctic delta but fail to depict the

481   heterogeneity of habitats and plant communities not only because of its coarse spatial resolution but

482   also because of the broad class descriptions. Furthermore, smaller areas are classified as 'tree

483   cover', 'needleleaved', 'evergreen / deciduous', 'closed to open (>15%)' and 'mosaic tree and shrub

484   (>50%) / herbaceous cover (<50%)' which is an inaccurate depiction of the delta.

485   This habitat map and the land cover classification from Schneider et al. (2009) resemble each other

486   more closely, however, this habitat map shows more differentiation in the classes and spatial

487   resolution, 10 m to 30 m, respectively. The only class description that is identical in both

488   classifications, besides water and sand / mainly non-vegetated areas, is 'dry tussock tundra'.

489   However, there is only a small match between these classes in the point comparison and most 'dry

490   tussock tundra' areas from the Schneider et al. (2009) classification fall into the PC_50%:, PC_20%,

491   'moist wet sedge complex' and 'dwarf shrub-herb communities'. The habitat map shows the mosaic

492   of habitats on the floodplain with 'moist equisetum and shrubs on floodplain', 'dry low shrub

493   community', 'moist to wet sedge' and 'wet sedge complex' which match with 'moist to dry dwarf

494   shrub-dominated tundra' in the land cover classification of Schneider et al. (2009). Also, for the

495   polygonal tundra complex, our habitat map shows more differentiation with three classes of up to

496   50% 20% 10% surface water contribution versus two classes in Schneider et al. (2009) 'wet sedge

497   and moss dominated tundra' and 'moist grass and moss dominated tundra' The areas covered by

498   'PC_50%' and 'PC_20%' match with 'wet sedge- and moss-dominated tundra', and 'PC_20%' and

499   'PC_10%' match with 'moist grass and moss-dominated tundra'. The overall aim of both maps is to

500   differentiate between dry to wet land cover habitats as these describe the heterogeneity in the delta

501   well and determine factors related to methane emissions (see Schneider et al. 2009) and the

502   different habitat classes.

503   The land cover classification from ESA GlobPermafrost differentiates between 21 classes which are

504   associated to eight broader groups, such as sparse vegetation, shrub tundra, forest, grassland,

505   floodplain, disturbed, barren and water (Bartsch et al., 2019). With a spatial resolution of 20 m, the

506   latter product is the closest to this habitat map. The major class 'wet ecotopes' of ESA

16

507   GlobPermafrost match with our 'PC_50%:' on the first terrace and the 'moist to wet sedge complex'
508   on the floodplains. On the floodplain however, other classes show less agreement. The ESA
509   GlobPermafrost one class 'floodplain mostly fluvial' does not differentiate the floodplain classes
510   further, in contrast to our habitat map differentiating between 'moist to wet sedge complex', 'wet
511   sedge complex', 'moist equisetum and shrubs' and 'dry low shrub community' on floodplain.
512   Whereas the ESA GlobPermafrost class 'disturbed' (defined as forest fire scars, seasonally
513   inundation and landslide scars can be found in 'PC_50%' predominantly, in 'sand', 'PC_20%' and
514   'sparsely vegetated areas' in our habitat map. This underlines the complex structure of match and
515   mismatch between classifications.

516   The land cover map from Schneider et al. (2009) is based on two cloud-free Landsat images from
517   June/July 2000 and 2001, the ESA CCI land cover 2018 map is based on summer images as well.
518   Hence, the images used for this habitat classification were acquired at a similar time as for the ESA
519   CCI product and we do not expect differences based on changes on the ground due to this temporal
520   concurrence. In the almost 20-year difference between Schneider et al. (2009) and this habitat map
521   we do expect changes in vegetation composition. Overall, it is challenging to obtain sufficient cloud-
522   free images during the summer months to fully cover the entire Lena Delta for a classification project
523   and to depict a specific phenological state. Therefore, we created a Sentinel-2 composite mosaic
524   based on the maximum NDVI value per pixel from June to September. With this we ensure to have
525   the peak vegetation and phenology season represented as input for the habitat classification as
526   much as possible and increase comparability to other classification studies despite a temporal
527   mismatch.

528   The habitat map gives an accurate and detailed description of the Arctic Lena Delta that
529   incorporates extensive field data and expert knowledge. The habitat map is superior to the ESA CCI
530   land cover map (2018) in both spatial resolution and class description as it depicts the
531   heterogeneous habitat distribution. The 20m ESA GlobPermafrost classification matches the
532   resolution of the habitat map closely but due to its wider geographical application with circum-Arctic
533   standardized classes it does not optimally represent Lena Delta-specific habitats, such as the widely
534   distributed polygonal tundra complex. Furthermore, the habitat map is an update to Schneider et al.
535   (2009), which was based on three Landsat images from 2000 and 2001 and shows further
536   differentiation of habitats, specifically representing the floodplain mosaics of this Arctic delta.

537   **4.3 Habitat linked disturbance regimes**

538   Parts of the Lena Delta are characterised by disturbances due to annual floodings or rapid
539   permafrost thaw processes leading to specific habitat classes. We provide habitat linked disturbance

17

540   regimes (describing the type and intensity of disturbances) across the delta. Our product (Dataset 6,

541   Figure 6a) shows that the largest part of the vegetated delta (excluding 12 439 km^2 of 'sand' and

542   'water' classes) is impacted by low disturbance, resulting in mature-state plant communities on the

543   terrace plateaus (Figure 6b, 72%, 12 806 km^2). Specifically, the second terrace in the northwest of

544   the delta, with low ice content, is least impacted by rapid thaw processes and not part of the active

545   delta. In contrast, the habitats in the active delta are all linked to high disturbance (27%, 4 875 km^2).

546   The 'moist to wet sedge complex' (10% of the vegetated Lena Delta) is the largest class considered

547   to be formed by high disturbance. This class is found in larger patch sizes on the riverine floodplains,

548   smaller patches on the floor of thermo-erosional valleys. Overall, 27.5% of the vegetated area of the

549   Lena Delta experiences some level of high disturbance from either regular spring floods or from

550   rapid thaw processes.

551   Species richness, relative abundance and biomass characteristics are important habitat features that

552   are influenced by landscape characteristics such as topography, water fluxes, soil types and

553   disturbance regimes (Forman and Godron, 1981; Naiman et al., 1986; Pickett et al., 1989;

554   Montgomery, 1999). Greig-Smith (1964), Woodwell and Whittaker (1968), and Forman and Godron

555   (1981) described fragmentation of land surfaces due to disturbance (defined by type and intensities)

556   and topography. In the Lena Delta, the terrace-related topography and active floodplain areas are

557   major determinants of plant communities and habitat classes and are thus well reflected in the Lena

558   Delta habitat map.

559   The high disturbance regime on floodplains results in 'shifting habitats' (Stanford et al., 2005; Driscoll

560   and Hauer, 2019). The annual spring floods and rapid thaw processes result in areas of high

561   disturbances, habitats of mid to advanced plant successional stages showing high vascular plant

562   above ground biomass (Figure 6c) due to the higher nutrient availability, a deeper active layer and

563   more moisture (e.g., Myers-Smith et al., 2020). Within the low disturbance habitat classes, a thick

564   moss layer as well as a low vascular plant coverage characterise the tundra community

565   assemblages representing mature state plant communities. Because high disturbance patches are

566   characterized by high vascular biomass, they can be well classified specifically in the NDVI, but also

567   NIR and red edge bands of optical medium resolution sensors such as S-2. Within the vegetation

568   plots (Dataset 1), we did not find clear differences in species richness and in the Shannon diversity

569   index between the disturbed and the undisturbed classes (Figure 6d). Since most disturbed habitat

570   classes such as the 'moist to wet sedge', the 'wet sedge' as well as homogeneous patches of high

571   shrubs (as part of the habitat class 'dry grass to wet sedge complex'), were not sampled in the field

572   due to too challenging conditions, however they are clearly representing habitats with low species

573   richness. In the extreme case disturbance can lead to barren and sparsely vegetated surfaces.

18

4.4 Classification accuracy and representativeness

574

575 The field data was acquired during a field trip in July-August 2018, primarily focusing on 30 m x 30 m
576 homogeneous vegetation and land cover plots. Additionally, we relied on Sentinel-2 images for the
577 different classifications that were also acquired in summer 2018, covering the same period as the
578 field trip, and have a spatial resolution of 20 m. The temporal overlap of the field work and the
579 satellite image acquisitions ensures consistency across the different datasets and represents a close
580 relationship between datasets and products obtained in the field (dataset 1, 2 and 3) and the results
581 derived from the satellite images that use the field data as input. As Sentinel-2 images have a small
582 geolocation error, we could link our field plot locations directly with the satellite images. Furthermore,
583 the sampling and measurement design of the plots with 30 m x 30 m ensured a reliable link to the
584 satellite data with similar spatial resolution, as we followed the recommendations on ESU. The
585 RGBNIR Sentinel-2 bands have a spatial resolution of 10 m and the red edge (NIR) and SWIR
586 bands a spatial resolution of 20 m, and even if we downsampled the bands to 10 m the spectral
587 information is sustained. More information on datasets and their spatial and temporal resolutions are
588 provided in supplementary Table S3.

589 The presented datasets are limited by the regional in-situ observations and expert knowledge
590 collected mainly in the central Lena Delta. The remoteness of the area and extremely difficult
591 logistics to conduct research in the second terrace and the outer rims of the delta are major reasons
592 for these limitations. However, the delta is relatively homogeneous in habitat classes that develop
593 based on underlying geomorphology and the disturbance regime (annual flooding and permafrost
594 thaw processes). Only one major habitat class is absent from the well studied central Lena Delta and
595 only occurs across the second terrace. Thus, even though detailed knowledge and in-situ
596 observations are derived from a relatively small subset of the Delta, we are confident that our
597 mapping results from the entire region are valuable and accurate. Also due to the inaccessibility of
598 large areas of the delta, quantitative accuracy assessments of the classifier and the final mapping
599 product are lacking. We had to rely on qualitative evaluation procedures by experts. Analysis of
600 similarity of habitat classes and S-2 spectral reflectance as well as NDVI values provide additional
601 quantitative and qualitative assessments on the extent to which the different classes are identifiable
602 and separated between classes.

603 In-situ observations (Datasets 1-3) as well as mapping products (Datasets 4-6) represent conditions
604 and vegetation composition of 2018. The timing of the summer 2018 expedition coincided with a
605 relatively high number of cloud free S-2 images necessary for a high quality habitat classification.
606 Overall, the described datasets are of appropriate quality to serve as a basis for additional studies
607 and most importantly as a baseline to identify changes in the future.

19

5 Conclusions

The described datasets provide coherent and complementary information of the major habitat classes in the Lena Delta in Arctic Siberia, the largest delta in the Arctic. Based on extensive knowledge collected during fieldwork that included habitat-related measurements of plant composition, biomass, and hyperspectral field measurements we provide a validated and high-resolution habitat classification map of the delta. In addition, we linked ecologically important characteristics of disturbances in the delta to habitat classes, providing a baseline for future studies of Arctic change as well as a foundation for potential upscaling of related processes such as biodiversity, ecosystem functions, and biochemical dynamics such as greenhouse gas emissions. With this update of previous land cover and habitat-related mapping products of the Lena Delta we strive to facilitate and promote future investigations leading to a better understanding of this highly sensitive arctic delta system.

Acknowledgements

Code/Data availability

Dataset 1: Shevtsova et al., 2021a, https://doi.pangaea.de/10.1594/PANGAEA.935875, Foliage projective cover of 26 vegetation sites in the central Lena Delta from 2018, is published as Foliage projective cover for all major taxa estimated as percent, as tab-delimited text files.

Dataset 2: Shevtsova et al., 2021b, https://doi.pangaea.de/10.1594/PANGAEA.935923, Total above-ground biomass of 25 vegetation sites in the central Lena Delta from 2018, is published as biomass aboveground dry mass per major taxa, as well as for 'moss and lichen', 'litter' and the remaining minor taxa (called 'other plants') and the total biomass in the units [g/m2], as tab-delimited text.

Dataset 3: Runge et al., 2022, https://doi.pangaea.de/10.1594/PANGAEA.945982, Hyperspectral field spectrometry of Arctic vegetation units in the central Lena Delta, is published as an overview of the plot details and field spectrometer reflectance spectra in the unit [%] of 28 vegetation plots, as tab-delimited text files.

20

636 Dataset 4: Landgraf et al., 2022 a,b,c. The Sentinel-2-derived central Lena Delta land cover (habitat)

637 classification consists of the following three data publications: i) Landgraf et al. 2022a,

638 https://doi.pangaea.de/10.1594/PANGAEA.945056: a raster file with assigned land cover classes and an

639 ESRI polygon shape file containing the 10 training classes representing the different vegetation

640 compositions, as geotiff file. Both datasets are based on 2018 satellite images and informed by the in-

641 situ vegetation plots and expert knowledge. Datasets are in Universe Transverse Mercator (UTM) Zone

642 52 North projection. ii) Landgraf et al. 2022b, https://doi.pangaea.de/10.1594/PANGAEA.945054. This

643 data set includes training elements representing different vegetation composition in the form of

644 Elementary Sampling Units ESUs: 69 pseudo ESUs set with expert knowledge from the field and from

645 Lena Delta expedition field reports. iii) Landgraf et al. 2022c,

646 https://doi.pangaea.de/10.1594/PANGAEA.945055. This data set includes training elements representing

647 different vegetation composition in the form of Elementary Sampling Units ESUs: 23 true ESUs

648 representing the LD18 vegetation plots.

649 Dataset 5: Lisovski et al., 2022, https://doi.pangaea.de/10.1594/PANGAEA.946407. The Lena Delta

650 Habitat Map (2018, Sentinel-2) contains i) the Lena Delta habitat map (13 classes), ii) the sand probability

651 map, both as geotiff files in WGS84 geographic projection, iii) the habitat class description as comma

652 delimited csv table, and iv) the training dataset (n = 4 278 classified pixels) in geographic decimal

653 coordinates comma delimited csv table. The data collection also contains the Lena Delta Region of

654 Interest (ROI) ESRI shapefile outlining the Lena Delta including a coastal water buffer.

655 Dataset 6: Heim and Lisovski, 2023, https://doi.org/10.5281/zenodo.7575691. The Lena Delta habitat

656 disturbance regime map is published in the form of two geotiff files (tiles) in WGS84 geographic

657 projection.

658 Code developed in Google Earth Engine to derive habitat classes based in the central Lena Delta

659 classification, as well as R code for figures can be accessed from the following repository: Lisovski,

660 S. (2024). Code for 'A new habitat map of the Lena Delta in Arctic Siberia based on field and remote

661 sensing datasets'. V0.1. Zenodo. 10.5281/zenodo.11197641.

Competing interests

663 Birgit Heim is a member of the editorial board of ESSD. Otherwise, we declare no competing interests.

21

Funding

Authors contribution

SL: Conceptual framework, habitat classification, data analysis, writing

AR: Conceptual framework, field work, spectral field data collection, habitat classification, spectral data processing, data analysis, writing

IS: Field work, biomass and projective cover measurement in vegetation plots, habitat classification

RRO: Habitat classification

NL: habitat classification, spectral data processing

MF: Field work, spectral field data collection

NiL: habitat class definition, field work

AM: Project management, writing

CS: Spectral data processing

AB: Spectral data processing

UH: Conceptual framework, project management

GG: Conceptual framework, project management, habitat classification, writing

BH: Conceptual framework, field work, habitat classification, project management, writing

22

Appendix
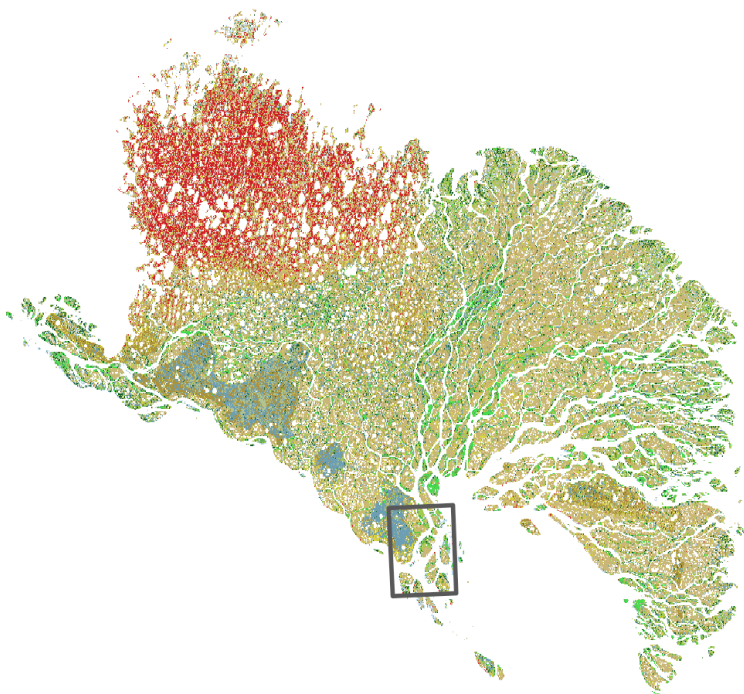
Figure A1: *Location of the central Lena Delta (Dataset 4) in the Lena Delta (Dataset 5,6). WGS 84 projection.*
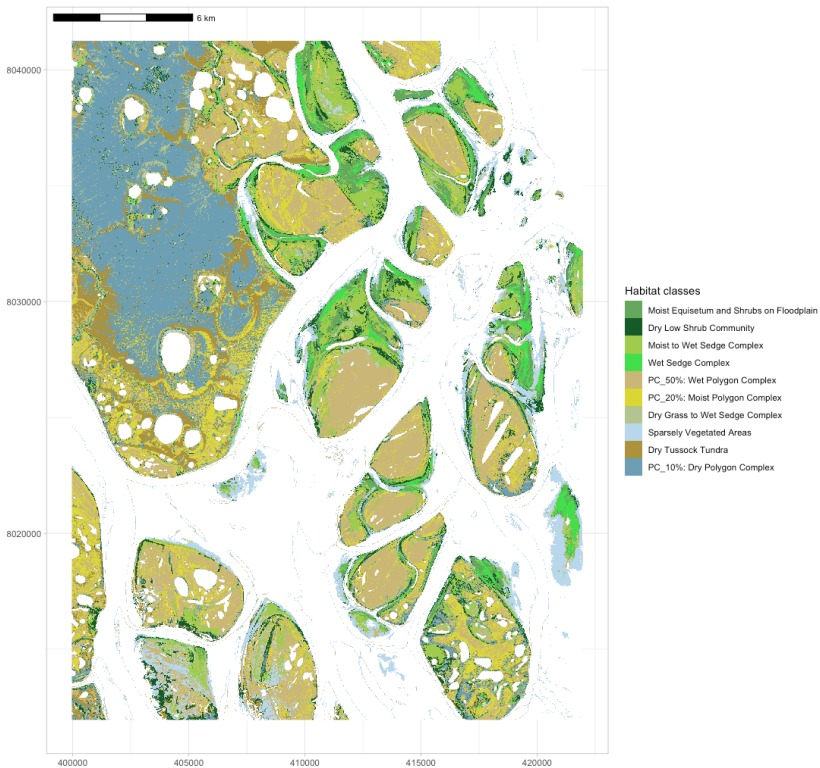
688
689

Figure A2: *Supervised habitat classification of the central Lena Delta based on a cloud-free S-2 August 2018 acquisition (Dataset 4). Numbers in legend correspond to the labels in published Dataset 4 (Landgraf et al. 2022). Universe Transverse Mercator Z52 on WGS 84 projection.*
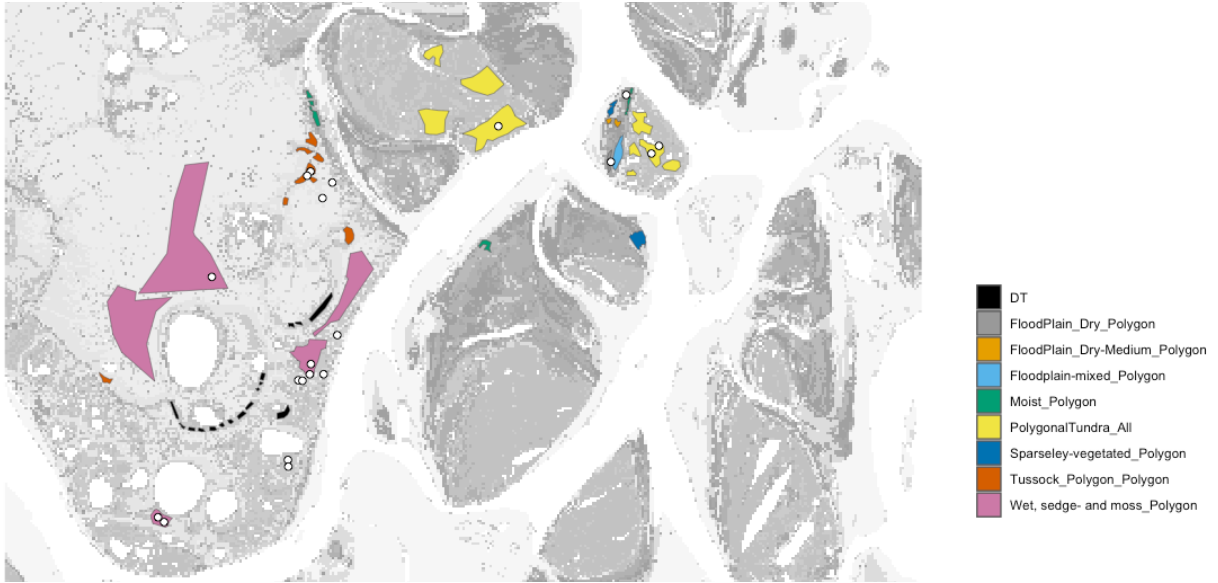
23

711

Figure A3: *Subset of the central Lena Delta with 30 x 30 m ESUs (white points, dataset 1) and polygons defined by expert knowledge (published with dataset 4). Together the ESUs and polygons served areas to sample 8 626 training pixels for the central Lena Delta landcover/habitat classification (dataset 4, Landgraf et al. 2022a).*
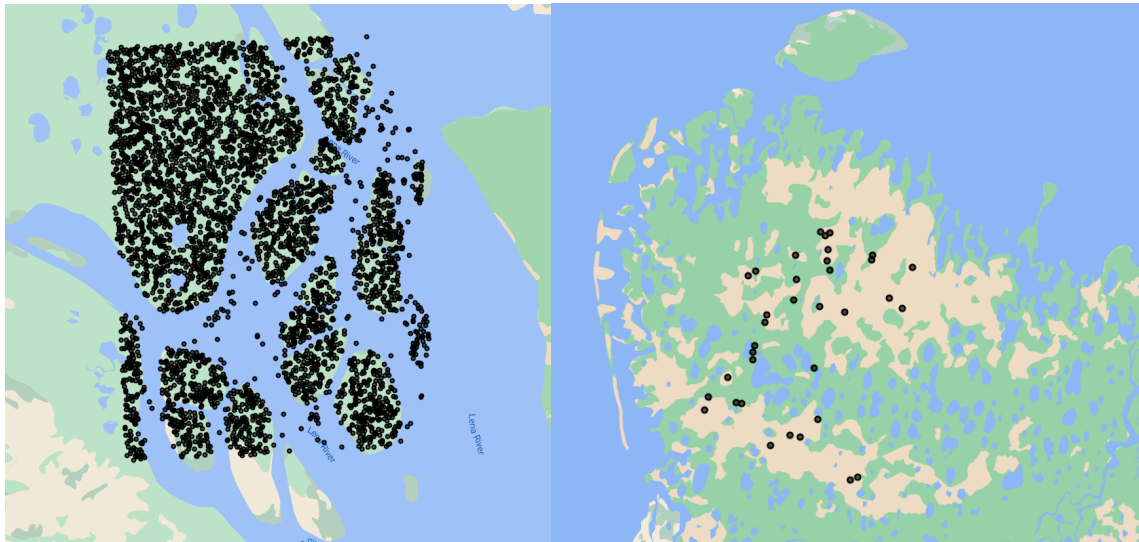

Figure A4: *Training pixels for the Lena Delta habitat classification (dataset 5). (Left) 7.500 random pixels samples across the habitat classes from the central Lena Delta landcover/habitat map (dataset 4). (Right) 35 pixels selected by expert knowledge for the 'dwarf shrub - herb communities' that are missing in the central Lena Delta.*

24

References

AMAP: AMAP Arctic Climate Change Update 2021: Key Trends and Impacts. Arctic Monitoring and Assessment Programme (AMAP), Tromsø, Norway, viii+148pp, 2021.

Bartlett, K. B., Crill, P. M., Sass, R. L., Harriss, R. C., and Dise, N. B.: Methane Emissions from Tundra Environments in the Yukon-Kuskokwim Delta, Alaska, Journal of Geophysical Research-Atmospheres, 97, 16645-16660, doi: 10.1029/91jd00610, 1992.

Bartsch, A., Hofler, A., Kroisleitner, C., and Trofaier, A. M.: Land Cover Mapping in Northern High Latitude Permafrost Regions with Satellite Data: Achievements and Remaining Challenges, Remote Sensing, 8, 979. doi: 10.3390/rs8120979, 2016.

Bartsch, A., Widhalm, B., Pointner, G., Ermokhina, K., Leibman, M., and Heim, B.: Landcover derived from Sentinel-1 and Sentinel-2 satellite data (2015-2018) for subarctic and arctic environments [dataset], https://doi.org/10.1594/PANGAEA.897916, 2019.

Bartsch, A., Widhalm, B., Leibman, M., Ermokhina, K., Kumpula, T., Skarin, A., Wilcox, E. J., Jones, B. M., Frost, G. V., Hofler, A., and Pointner, G.: Feasibility of tundra vegetation height retrieval from Sentinel-1 and Sentinel-2 data, Remote Sensing of Environment, 237, 111515, doi: 10.1016/j.rse.2019.111515, 2020.

Beamish, A., Raynolds, M. K., Epstein, H., Frost, G. V., Macander, M. J., Bergstedt, H., Bartsch, A., Kruse, S., Miles, V., Tanis, C. M., Heim, B., Fuchs, M., Chabrillat, S., Shevtsova, I., Verdonen, M., and Wagner, J.: Recent trends and remaining challenges for optical remote sensing of Arctic tundra vegetation: A review and outlook, Remote Sensing of Environment, 246, ARTN 111872, doi: 10.1016/j.rse.2020.111872, 2020.

Beamish, A. L., Coops, N., Chabrillat, S., and Heim, B.: A Phenological Approach to Spectral Differentiation of Low-Arctic Tundra Vegetation Communities, North Slope, Alaska, Remote Sensing, 9, 1200, doi: 10.3390/rs9111200, 2017.

Beamish, A. L., Coops, N. C., Hermosilla, T., Chabrillat, S., and Heim, B.: Monitoring pigment-driven vegetation changes in a low-Arctic tundra ecosystem using digital cameras, Ecosphere, 9, e02123, doi: 10.1002/ecs2.2123, 2018.

Berner, L. T., Massey, R., Jantz, P., Forbes, B. C., Macias-Fauria, M., Myers-Smith, I., Kumpula, T., Gauthier, G., Andreu-Hayles, L., Gaglioti, B. V., Burns, P., Zetterberg, P., D'Arrigo, R., and Goetz, S. J.: Summer warming explains widespread but not uniform greening in the Arctic tundra biome, Nature Communications, 11, 4621, doi: 10.1038/s41467-020-18479-5, 2020.

Biskaborn, B. K., Smith, S. L., Noetzli, J., Matthes, H., Vieira, G., Streletskiy, D. A., Schoeneich, P., Romanovsky, V. E., Lewkowicz, A. G., Abramov, A., Allard, M., Boike, J., Cable, W. L., Christiansen, H. H., Delaloye, R., Diekmann, B., Drozdov, D., Etzelmuller, B., Grosse, G., Guglielmin, M., Ingeman-Nielsen, T., Isaksen, K., Ishikawa, M., Johansson, M., Johannsson, H., Joo, A., Kaverin, D., Kholodov, A., Konstantinov, P., Kroger, T., Lambiel, C., Lanckman, J. P., Luo, D. L., Malkova, G., Meiklejohn, I., Moskalenko, N., Oliva, M., Phillips, M., Ramos, M., Sannel, A. B. K., Sergeev, D., Seybold, C., Skryabin, P., Vasiliev, A., Wu, Q. B., Yoshikawa, K., Zheleznyak, M., and Lantuit, H.: Permafrost is warming at a global scale, Nature Communications, 10, 264, doi: 10.1038/s41467-018-08240-4, 2019.

Boike, J., Wille, C., and Abnizova, A.: Climatology and summer energy and water balance of polygonal tundra in the Lena River Delta, Siberia, Journal of Geophysical Research-Biogeosciences, 113, G03025, doi: 10.1029/2007jg000540, 2008.

Boike, J., Nitzbon, J., Anders, K., Grigoriev, M., Bolshiyanov, D., Langer, M., Lange, S., Bornemann, N., Morgenstern, A., Schreiber, P., Wille, C., Chadburn, S., Gouttevin, I., Burke, E., and Kutzbach, L.: A 16-year record (2002-2017) of permafrost, active-layer, and meteorological conditions at the Samoylov Island Arctic permafrost research site, Lena River delta, northern Siberia: an opportunity to validate remote-sensing data and land surface, snow, and permafrost models, Earth System Science Data, 11, 261-299, doi: 10.5194/essd-11-261-2019, 2019.

Box, J. E., Colgan, W. T., Christensen, T. R., Schmidt, N. M., Lund, M., Parmentier, F. J. W., Brown, R., Bhatt, U. S., Euskirchen, E. S., Romanovsky, V. E., Walsh, J. E., Overland, J. E., Wang, M. Y., Corell, R. W., Meier, W. N., Wouters, B., Mernild, S., Mard, J., Pawlak, J., and Olsen, M. S.: Key indicators of Arctic climate change: 1971-2017, Environmental Research Letters, 14, 045010, doi: 10.1088/1748-9326/aafc1b, 2019.

Buchhorn, M., Walker, D. A., Heim, B., Raynolds, M. K., Epstein, H. E., and Schwieder, M.: Ground-Based Hyperspectral Characterization of Alaska Tundra Vegetation along Environmental Gradients, Remote Sensing, 5, 3971-4005, doi: 10.3390/rs5083971, 2013.

780   Driscoll, K. P. and Hauer, F. R.: Seasonal flooding affects habitat and landscape dynamics of a
781   gravel-bed river floodplain, Freshwater Science, 38, 510-526, doi: 10.1086/704826, 2019.

782   Drusch, M., Del Bello, U., Carlier, S., Colin, O., Fernandez, V., Gascon, F., Hoersch, B., Isola,
783   C., Laberinti, P., Martimort, P., Meygret, A., Spoto, F., Sy, O., Marchese, F., Bargellini, P.,
784   Sentinel-2: ESA's optical high-resolution mission for GMES operational services. Rem. Sens.
785   Environ., 120, 25–36, doi: 10.1016/j.rse.2011.11.026 , 2012.

786   Duncanson, L., Armston, J., Disney, M., Avitabile, V., Barbier, N., Calders, K., Carter, S.,
787   Chave, J., Herold, M., MacBean, N., McRoberts, R., Minor, D., Paul, K., Réjou-Méchain, M.,
788   Roxburgh, S., Williams, M., Albinet, C., Baker, T., Bartholomeus, H., Bastin, J. F., Coomes, D.,
789   Crowther, T., Davies, S., de Bruin, S., De Kauwe, M., Domke, G., Dubayah, R., Falkowski, M.,
790   Fatoyinbo, L., Goetz, S., Jantz, P., Jonckheere, I., Jucker, T., Kay, H., Kellner, J., Labriere, N.,
791   Lucas, R., Mitchard, E., Morsdorf, F., Næsset, E., Park, T., Phillips, O. L., Ploton, P., Puliti, S.,
792   Quegan, S., Saatchi, S., Schaaf, C., Schepaschenko, D., Scipal, K., Stovall, A., Thiel, C.,
793   Wulder, M. A., Camacho, F., Nickeson, J., Román, M., and Margolis, H.: Aboveground Woody
794   Biomass Product Validation Good Practices Protocol. Version 1.0, Land Product Validation
795   Subgroup (WGCV/CEOS), doi:10.5067/doc/ceoswgcv/lpv/agb.001, 2021.

796   Endsley, K. A., Kimball, J. S., and Reichle, R. H.: Soil Respiration Phenology Improves Modeled
797   Phase of Terrestrial net Ecosystem Exchange in Northern Hemisphere, Journal of Advances in
798   Modeling Earth Systems, 14, e2021MS002804, doi: 10.1029/2021MS002804, 2022.

799   ESA, 2015. Sentinel-2 User Handbook. ESA Standard Document.

800   ESA Land Cover CCI project team; Defourny, P. (2019): ESA Land Cover Climate Change
801   Initiative (Land_Cover_cci): Global Land Cover Maps, Version 2.0.7. Centre for
802   Environmental Data Analysis, *downloaded 2022,* [dataset]
803   https://catalogue.ceda.ac.uk/uuid/b382ebe6679d44b8b0e68ea4ef4b701c

804   Fedorova, I., Chetverova, A., Bolshiyanov, D., Makarov, A., Boike, J., Heim, B., Morgenstern,
805   A., Overduin, P. P., Wegner, C., Kashina, V., Eulenburg, A., Dobrotina, E., and Sidorina, I.:
806   Lena Delta hydrology and geochemistry: long-term hydrological data and recent field
807   observations, Biogeosciences, 12, 345-363, doi: 10.5194/bg-12-345-2015, 2015.

27

808   Forman, R. T. T. and Godron, M.: Patches and Structural Components for a Landscape

809   Ecology, Bioscience, 31, 733-740, doi 10.2307/1308780, 1981.

810   Frost, G. V., Loehman, R. A., Saperstein, L. B., Macander, M. J., Nelson, P. R., Paradis, D. P.,

811   and Natali, S. M.: Multi-decadal patterns of vegetation succession after tundra fire on the

812   Yukon-Kuskokwim Delta, Alaska, Environmental Research Letters, 15, 025003, doi:

813   10.1088/1748-9326/ab5f49, 2020.

814   Gilg, O., Sané, R., Solovieva, D. V., Pozdnyakov, V. I., Sabard, B., Tsanos, D., Zöckler, C.,

815   Lappo, E. G., Syroechkovski, J. E. E., and Eichhorn, G.: Birds and Mammals of the Lena Delta

816   Nature Reserve, Siberia, ARCTIC, 53, 118-133, doi: 10.14430/arctic842, 2000.

817   Greig-Smith, P.: Quantitative plant ecology, Butterworths1964.

818   Grigoriev, M. N.: Crio Morphogenesis in the Lena Delta, Permafrost Institute Press, Yakutsk

819   1993.

820   Heim, B. and Lisovski, S.: Lena Delta habitat disturbance regimes (0.0) [dataset], Zenodo,

821   https://doi.org/10.5281/zenodo,7575691, 2023.

822   Holl, D., Wille, C., Sachs, T., Schreiber, P., Runkle, B. R. K., Beckebanze, L., Langer, M., Boike,

823   J., Pfeiffer, E. M., Fedorova, I., Bolshianov, D. Y., Grigoriev, M. N., and Kutzbach, L.: A long-

824   term (2002 to 2017) record of closed-path and open-path eddy covariance CO_2 net ecosystem

825   exchange fluxes from the Siberian Arctic, Earth System Science Data, 11, 221-240, doi:

826   10.5194/essd-11-221-2019, 2019.

827   Hu, F. S., Higuera, P. E., Duffy, P., Chipman, M. L., Rocha, A. V., Young, A. M., Kelly, R., and

828   Dietze, M. C.: Arctic tundra fires: natural variability and responses to climate change, Frontiers

829   in Ecology and the Environment, 13, 369-377, doi: 10.1890/150063, 2015.

830   Hubberten, H.-W., Wagner, D., Pfeiffer, E.-M., Boike, J., and Gukov, A. Y.: The Russian-

831   German research station samoylov, Lena delta -A key site for polar research in the Siberian

832   arctic, Polarforschung, 2006.

833   Jorgenson, M. T.: Hierarchial organisation of ecosystems at multiple spatial scales on the

834   Yukon-Kuskokwim Delta, Alaska, USA, Arctic Antarctic and Alpine Research, 32, 221-239, doi

835   10.2307/1552521, 2000.

836 Juhls, B., Antonova, S., Angelopoulos, M., Bobrov, N., Grigoriev, M., Langer, M., Maksimov, G.,

837 Miesner, F., and Overduin, P. P.: Serpentine (Floating) Ice Channels and their Interaction with

838 Riverbed Permafrost in the Lena River Delta, Russia, Frontiers in Earth Science, 9, 689941, doi:

839 10.3389/feart.2021.689941, 2021.

840 Kienast, F. and Tsherkasova, J.: Comparative botanical recent-studies in the Lena River Delta

841 [Field Report], Alfred Wegener Institute, Germany, 2001.

842 Landgraf, N., Shevtsova, I., Pflug, B., and Heim, B. .: Sentinel-2 derived central Lena Delta land

843 cover classification, PANGAEA [dataset], https://doi.pangaea.de/10.1594/PANGAEA.945057,

844 2022a.

845 Landgraf, N., Shevtsova, I., Pflug, B., and Heim, B.: Raster file with assigned land cover classes

846 and ESRI polygon shape file training classes representing different vegetation composition,

847 PANGAEA [dataset], https://doi.pangaea.de/10.1594/PANGAEA.945056, 2022b.

848 Landgraf, N., Shevtsova, I., Pflug, B., and Heim, B.: 23 true Elementary Sampling Units (ESUs)

849 set in the Lena Delta representing the LD18 vegetation plots, PANGAEA [dataset],

850 https://doi.pangaea.de/10.1594/PANGAEA.945055, 2022c.

851 Landgraf, N., Shevtsova, I., Pflug, B., and Heim, B.: 69 pseudo Elementary Sampling Units

852 (ESUs) set in the Lena Delta derived with expert knowledge, PANGAEA [dataset],

853 https://doi.pangaea.de/10.1594/PANGAEA.945054, 2022d.

854 Lantz, T. C., Kokelj, S. V., and Fraser, R. H.: Ecological recovery in an Arctic delta following

855 widespread saline incursion, Ecological Applications, 25, 172-185, doi: 10.1890/14-0239.1,

856 2015.

857 Lisovski, S., Runge, A., Okoth, R. R., Shevtsova, I., and Heim, B.: Lena Delta Land Cover

858 Classification (2018, Sentinel-2), PANGAEA [dataset], doi: 10.1594/PANGAEA.946407, 2022.

859 Lorang, M. S. and Hauer, F. R.: Fluvial geomorphic processes, in: Methods in stream ecology,

860 edited by: Hauer, F. R., and Lamberti, G. A., Academic Press/Elsevier, San Diego, 145–168,

861 2006.

862 Macander, M. J., Nelson, P. R., Nawrocki, T. W., Frost, G. V., Orndahl, K. M., Palm, E. C.,

863 Wells, A. F., and Goetz, S. J.: Time-series maps reveal widespread change in plant functional

864 type cover across Arctic and boreal Alaska and Yukon, Environmental Research Letters, 17,
865 ARTN 054042, doi: 10.1088/1748-9326/ac6965, 2022.

866 Mauclet, E., Agnan, Y., Hirst, C., Monhonval, A., Pereira, B., Vandeuren, A., Villani, M.,
867 Ledman, J., Taylor, M., Jasinski, B. L., Schuur, E. A. G., and Opfergelt, S.: Changing sub-Arctic
868 tundra vegetation upon permafrost degradation: impact on foliar mineral element cycling,
869 Biogeosciences, 19, 2333-2351, doi: 10.5194/bg-19-2333-2022, 2022.

870 Mekonnen, Z. A., Riley, W. J., Berner, L. T., Bouskill, N. J., Torn, M. S., Iwahana, G., Breen, A.
871 L., Myers-Smith, I. H., Criado, M. G., Liu, Y. L., Euskirchen, E. S., Goetz, S. J., Mack, M. C., and
872 Grant, R. F.: Arctic tundra shrubification: a review of mechanisms and impacts on ecosystem
873 carbon balance, Environmental Research Letters, 16, 053001, doi: 0.1088/1748-9326/abf28b,
874 2021.

875 Montgomery, D. R.: Process domains and the river continuum, Journal of the American Water
876 Resources Association, 35, 397-410, doi: 10.1111/j.1752-1688.1999.tb03598.x, 1999.

877 Morgenstern, A., Grosse, G., and Schirrmeister, L.: Genetic, morphological, and statistical
878 characterization of lakes in the permafrost-dominated Lena Delta, Ninth International
879 Conference on Permafrost, 2008.

880 Morgenstern, A., Grosse, G., Gunther, F., Fedorova, I., and Schirrmeister, L.: Spatial analyses
881 of thermokarst lakes and basins in Yedoma landscapes of the Lena Delta, Cryosphere, 5, 849-
882 867, doi:10.5194/tc-5-849-2011, 2011.

883 Morgenstern, A., Overduin, P. P., Gunther, F., Stettner, S., Ramage, J., Schirrmeister, L.,
884 Grigoriev, M. N., and Grosse, G.: Thermo-erosional valleys in Siberian ice-rich permafrost,
885 Permafrost and Periglacial Processes, 32, 59-75, doi: 10.1002/ppp.2087, 2021.

886 Morgenstern, A., Ulrich, M., Gunther, F., Roessler, S., Fedorova, I. V., Rudaya, N. A., Wetterich,
887 S., Boike, J., and Schirrmeister, L.: Evolution of thermokarst in East Siberian ice-rich
888 permafrost: A case study, Geomorphology, 201, 363-379, doi:
889 10.1016/j.geomorph.2013.07.011, 2013.

890 Mueller-Bombois, D. and Ellenberg, H.: Aims and methods of vegetation ecology, Wohn Wiley &
891 Sons, New York, USA1974.

892 Myers-Smith, I. H., Kerby, J. T., Phoenix, G. K., Bjerke, J. W., Epstein, H. E., Assmann, J. J.,
893 John, C., Andreu-Hayles, L., Angers-Blondin, S., Beck, P. S. A., Berner, L. T., Bhatt, U. S.,
894 Bjorkman, A. D., Blok, D., Bryn, A., Christiansen, C. T., Cornelissen, J. H. C., Cunliffe, A. M.,
895 Elmendorf, S. C., Forbes, B. C., Goetz, S. J., Hollister, R. D., de Jong, R., Loranty, M. M.,
896 Macias-Fauria, M., Maseyk, K., Normand, S., Olofsson, J., Parker, T. C., Parmentier, F. J. W.,
897 Post, E., Schaepman-Strub, G., Stordal, F., Sullivan, P. F., Thomas, H. J. D., Tommervik, H.,
898 Treharne, R., Tweedie, C. E., Walker, D. A., Wilmking, M., and Wipf, S.: Complexity revealed in
899 the greening of the Arctic, Nature Climate Change, 10, 106-117, doi: 10.1038/s41558-019-0688-
900 1, 2020.

901 Naiman, R. J., Melillo, J. M., and Hobbie, J. E.: Ecosystem Alteration of Boreal Forest Streams
902 by Beaver (Castor-Canadensis), Ecology, 67, 1254-1269, doi: 10.2307/1938681, 1986.

903 Nitzbon, J., Westermann, S., Langer, M., Martin, L. C. P., Strauss, J., Laboor, S., and BOike, J.:
904 Fast response of cold ice-rich permafrost in northeast Siberia to a warming climate, Nature
905 Communications, 11, 2201, doi: 10.1038/s41467-020-15725-8, 2020.

906 Nitze, I. and Grosse, G.: Detection of landscape dynamics in the Arctic Lena Delta with
907 temporally dense Landsat time-series stacks, Remote Sensing of Environment, 181, 27-41, doi:
908 10.1016/j.rse.2016.03.038, 2016.

909 Obu, J., Westermann, S., Barboux, C., Bartsch, A., Delaloye, R., Grosse, G., Heim, B.,
910 Hugelius, G., Irrgang, A., Kääb, A. M., Kroisleitner, C., Matthes, H., Nitze, I., Pellet, C., Seifert,
911 F. M., Strozzi, T., Wegmüller, U., Wieczorek, M., and Wiesmann, A.: ESA permafrost Climate
912 Change Initiative (permafrost_cci): Permafrost extent for the Northern Hemisphere, v2.0
913 [dataset], https://doi.org/10.5285/28E889210F884B469D7168FDE4B4E54F, 2020.

914 Overeem, I., Nienhuis, J. H., and Piliouras, A.: Ice-dominated Arctic deltas, Nature Reviews
915 Earth & Environment, 3, 225-240, doi: 10.1038/s43017-022-00268-x, 2022.

916 Overland, J., Dunlea, E., Box, J. E., Corell, R., Forsius, M., Kattsov, V., Olseng, M. S., Pawlak,
917 J., Reiersen, L. O., and Wang, M. Y.: The urgency of Arctic change, Polar Science, 21, 6-13,
918 doi: 10.1016/j.polar.2018.11.008, 2019.

919 Pickett, S. T. A., Kolasa, J., Armesto, J. J., and Collins, S. L.: The Ecological Concept of
920 Disturbance and Its Expression at Various Hierarchical Levels, Oikos, 54, 129-136, doi:
921 10.2307/3565258, 1989.

922   Piliouras, A. and Rowland, J. C.: Arctic River Delta Morphologic Variability and Implications for

923   Riverine Fluxes to the Coast, Journal of Geophysical Research-Earth Surface, 125, ARTN

924   e2019JF005250, doi: 10.1029/2019JF005250, 2020.

925   Pisaric, M. F. J., Thienpont, J. R., Kokelj, S. V., Nesbitt, H., Lantz, T. C., Solomon, S., and Smol,

926   J. P.: Impacts of a recent storm surge on an Arctic delta ecosystem examined in the context of

927   the last millennium, Proceedings of the National Academy of Sciences of the United States of

928   America, 108, 8960-8965, doi: 10.1073/pnas.1018527108, 2011.

929   Raynolds, M. K., Walker, D. A., Balser, A., Bay, C., Campbell, M., Cherosov, M. M., Daniels, F.

930   J. A., Eidesen, P. B., Emiokhina, K. A., Frost, G. V., Jedrzejek, B., Jorgenson, M. T., Kennedy,

931   B. E., Kholod, S. S., Lavrinenko, I. A., Lavrinenko, O. V., Magnusson, B., Matveyeva, N. V.,

932   Metusalemsson, S., Nilsen, L., Olthof, I., Pospelov, I. N., Pospelova, E. B., Pouliot, D.,

933   Razzhivin, V., Schaepman-Strub, G., Sibik, J., Telyatnikov, M. Y., and Troeva, E.: A raster

934   version of the Circumpolar Arctic Vegetation Map (CAVM), Remote Sensing of Environment,

935   232, ARTN 111297, doi: 10.1016/j.rse.2019.111297, 2019.

936   Romanovskii, N. N. and Hubberten, H. W.: Results of permafrost modelling of the lowlands and

937   shelf of the Laptev Sea region, Russia, Permafrost and Periglacial Processes, 12, 191-202, doi:

938   10.1002/ppp.387, 2001.

939   Rossger, N., Sachs, T., Wille, C., Boike, J., and Kutzbach, L.: Seasonal increase of methane

940   emissions linked to warming in Siberian tundra, Nature Climate Change, 12, 1031-+, doi:

941   10.1038/s41558-022-01512-4, 2022.

942   Runge, A., Fuchs, M., Shevtsova, I., Landgraf, N., Heim, B., Herzschuh, U., and Grosse, G.:

943   Hyperspectral field spectrometry of Arctic vegetation units in the central Lena Delta [dataset],

944   https://doi.org/10.1594/PANGAEA.945982, 2022.

945   Sachs, T., Wille, C., Boike, J., and Kutzbach, L.: Environmental controls on ecosystem-scale

946   CH4 emission from polygonal tundra in the Lena River Delta, Siberia, Journal of Geophysical

947   Research-Biogeosciences, 113, Artn G00a03, doi: 10.1029/2007jg000505, 2008.

948   Schirrmeister, L., Grosse, G., Schwamborn, G., Andreev, A. A., Meyer, H., Kunitsky, V. V.,

949   Kuznetsova, T. V., Dorozhkina, M. V., Pavlova, E. Y., Bobrov, A. A., and Oezen, D.: Late

950   Quaternary History of the Accumulation Plain North of the Chekanovsky Ridge (Lena Delta,

951 Russia): A Multidisciplinary Approach, Polar Geography, 27, 277-319, doi: 10.1080/789610225,
952 2003.

953 Schirrmeister, L., Grosse, G., Schnelle, M., Fuchs, M., Krbetschek, M., Ulrich, M., Kunitsky, V.,
954 Grigoriev, M., Andreev, A., Kienast, F., Meyer, H., Babiy, O., Klimova, I., Bobrov, A., Wetterich,
955 S., and Schwamborn, G.: Late Quaternary paleoenvironmental records from the western Lena
956 Delta, Arctic Siberia, Palaeogeography Palaeoclimatology Palaeoecology, 299, 175-196, doi:
957 10.1016/j.palaeo.2010.10.045, 2011.

958 Schneider, J., Grosse, G., and Wagner, D.: Land cover classification of tundra environments in
959 the Arctic Lena Delta based on Landsat 7 ETM+ data and its application for upscaling of
960 methane emissions, Remote Sensing of Environment, 113, 380-391, doi:
961 10.1016/j.rse.2008.10.013, 2009.

962 Schwamborn, G., Rachold, V., and Grigoriev, M. N.: Late Quaternary sedimentation history of
963 the Lena Delta, Quaternary International, 89, 119-134, doi: 10.1016/S1040-6182(01)00084-2,
964 2002.

965 Schwamborn, G., Schirrmeister, L., Mohammadi, A., Meyer, H., Kartoziia, A., Maggioni, F., and
966 Strauss, J.: Fluvial and permafrost history of the lower Lena River, north-eastern Siberia, over
967 late Quaternary time, Sedimentology, 70, 235-258, doi: 10.1111/sed.13037, 2023.

968 Serreze, M. C. and Barry, R. G.: Processes and impacts of Arctic amplification: A research
969 synthesis, Global and Planetary Change, 77, 85-96, doi: 10.1016/j.gloplacha.2011.03.004,
970 2011.

971 Shevtsova, I., Laschinskiy, N., Heim, B., and Herzschuh, U.: Foliage projective cover of 26
972 vegetation sites of central Lena Delta from 2018 [dataset],
973 https://doi.pangaea.de/10.1594/PANGAEA.935875, 2021a.

974 Shevtsova, I., Heim, B., Runge, A., Fuchs, M., Melchert, J., and Herzschuh, U.: Total above-
975 ground biomass of 25 vegetation sites of central Lena Delta from 2018 [dataset],
976 https://doi.pangaea.de/10.1594/PANGAEA.935923, 2021b.

977 Stanford, J. A., Lorang, M. S., and Hauer, F. R.: The shifting habitat mosaic of river ecosystems,
978 SIL Proceedings, 1922-2010, 29, 123-136, doi: 10.1080/03680770.2005.11901979, 2005.

979 Sweeney, C., Chatterjee, A., Wolter, S., McKain, K., Bogue, R., Conley, S., Newberger, T., Hu,

980 L., Ott, L., Poulter, B., Schiferl, L., Weir, B., Zhang, Z., and Miller, C. E.: Using atmospheric

981 trace gas vertical profiles to evaluate model fluxes: a case study of Arctic-CAP observations and

982 GEOS simulations for the ABoVE domain, Atmospheric Chemistry and Physics, 22, 6347-6364,

983 doi: 10.5194/acp-22-6347-2022, 2022.

984 Ulrich, M., Grosse, G., Chabrillat, S., and Schirrmeister, L.: Spectral characterization of

985 periglacial surfaces and geomorphological units in the Arctic Lena Delta using field spectrometry

986 and remote sensing, Remote Sensing of Environment, 113, 1220-1235, doi:

987 10.1016/j.rse.2009.02.009, 2009.

988 van Everdingen, R. O.: Multi-language glossary of permafrost and related ground-ice terms,

989 Arctic Institute of North America University of Calgary, Calgary, Canada1998.

990 Veremeeva, A. and Gubin, S.: Modern Tundra Landscapes of the Kolyma Lowland and their

991 Evolution in the Holocene, Permafrost and Periglacial Processes, 20, 399-406, doi:

992 10.1002/ppp.674, 2009.

993 Vulis, L., Tejedor, A., Zaliapin, I., Rowland, J. C., and Foufoula-Georgiou, E.: Climate

994 Signatures on Lake And Wetland Size Distributions in Arctic Deltas, Geophysical Research

995 Letters, 48, ARTN e2021GL094437, doi: 10.1029/2021GL094437, 2021.

996 Walker, H. J.: Arctic deltas, Journal of Coastal Research, 14, 718–738, 1998.

997 Whitaker, R. H. and Woodwell, G. M.: Dimension, and Production Relations of Trees and

998 Shrubs in the Brookhaven Forest, New York., Journal of Ecology, 56, 1-25, doi: 10.1038/2325,

999 1968.

1000 Zibulski, R., Herzschuh, U., and Pestryakova, L. A.: Vegetation patterns along micro-relief and

1001 vegetation type transects in polygonal landscapes of the Siberian Arctic, Journal of Vegetation

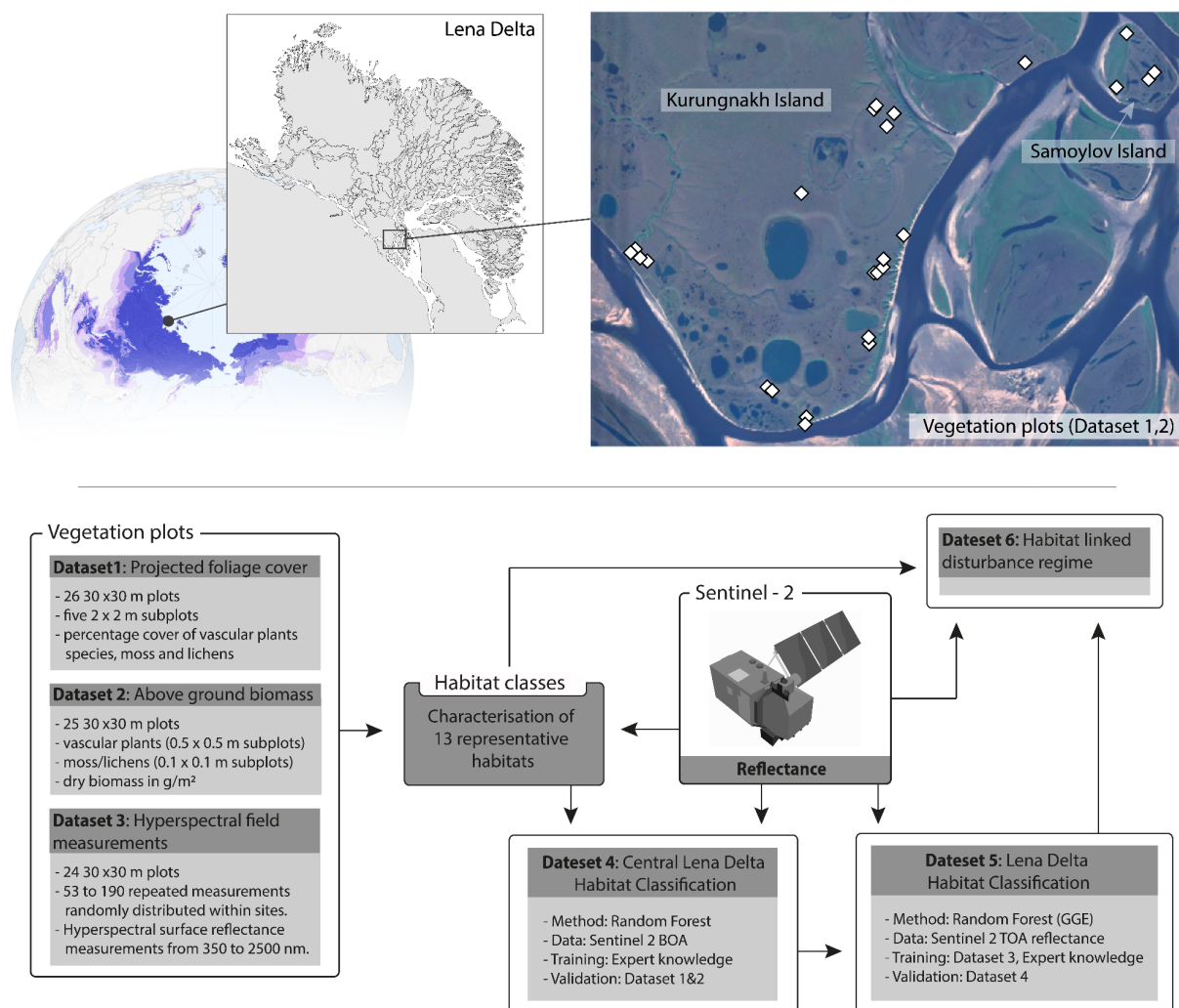1002 Science, 27, 377-386, doi: 10.1111/jvs.12356, 2016.

1003

Figures

Figure 1: Geographic location of the Lena Delta in the Russian High Arctic (72.91ºN, 126.90ºE) and a Sentinel-2 RGB image (August 2018, bands 4-3-2) of the central Lena Delta showing the areas of the 26 vegetation plots where foliage projective cover and above ground biomass was determined. Panarctic overview map shows permafrost extent (colour scale indicates permafrost extent from continuous (dark purple) to isolated (light purple) (Obu et al., 2020). The grey-coloured Lena Delta land map created with Sentinel-1 water mask from Juhls et al. (2021). Bottom: Dataset characteristics and methodological links between the different datasets.
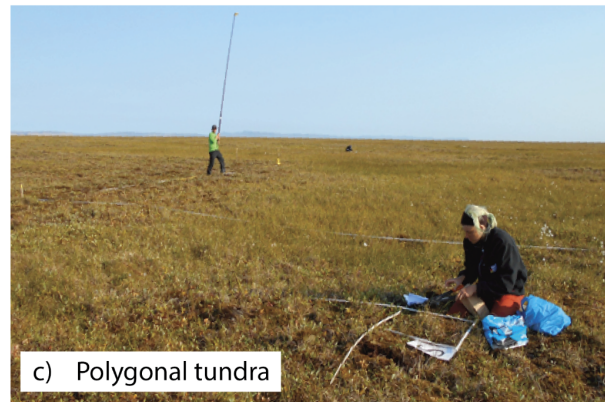
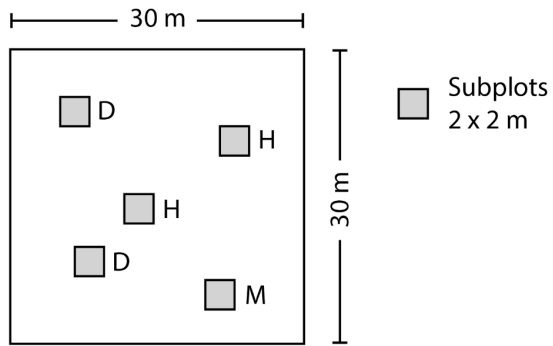Figure 2. Vegetation plots (30 x 30 m) were established in different vegetation types across the central Lena Delta. For subplots (2 x 2 m), the projective vegetation cover was recorded and labeled according to vegetation and moisture properties (H-Type: homogeneous, M-Type: moist, D-Type: dry). Figures illustrate example plots in a) tussock tundra (VP14), b) dry shrub communities (VP05), c) polygonal tundra (VP13). Photos: AWI.

Subplot
2 m

2 m

Biomass Plot
plot 0.5 x 0.5 m

b) Dry shrub community

T B
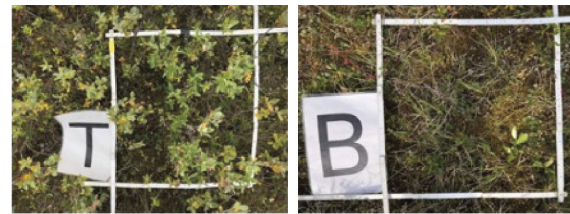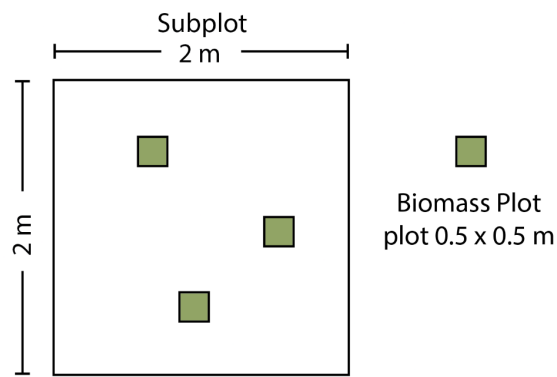
Wet biomass

Dry biomass

1020

1021   Figure 3. Biomass was sampled in subplots of 0.5 x 0.5 m (and 0.1 x 0.1 m for moss and
1022   lichens) distributed within the 2 x 2 m subplots described in Figure 2. Collected plants were
1023   weighted (wet biomass), dried in an oven and again weighted (dry biomass). Fotos: AWI.

1024

Figure 4: Similarity of habitat classes based on Sentinel-2 spectral reflectance and NDVI values. The dendrogram in panel a) indicates the multidimensional hierarchical similarity of the classes based on Sentinel-2 top of atmosphere reflectance (bands 2-8, 10-12, and NDVI). Panel b) shows the location of the habitat classes within a two-dimensional NMDS space. The arrows with the Sentinel-2 bands and NDVI indicate the correlation of these variables across the two axes. The lower matrix of panel c) depicts the calculated percentage overlap of 3,500 pixels (grey dots in panel b) across the two NMDS axes of panel b).

1032

Legend:
- Moist equi. and shrub comm.
- Dry low shrub communities
- Moist to wet sedge complex
- Wet sedge communities
- Polygonal tundra up to 50% surface water
- Polygonal tundra up to 20% surface water
- Dry grass to wet sedge complex
- Sparsely vegetated areas
- Dry tundra communities
- Polygonal tundra up to 10% surface water
- Dwarsh shrub - herb communities
- (Sand, Water)

Sand
(Percentage of Sentinal 2 scenes with cloud free pixel no water coverage and no vegetation)

5 %   80 %

1033

1034   Figure 5: Lena Delta habitat classes (Dataset 5). The entire Lena Delta on the left with three
1035   regional examples, showing (A) the seasonal sand probability and (B, C) regional examples of the
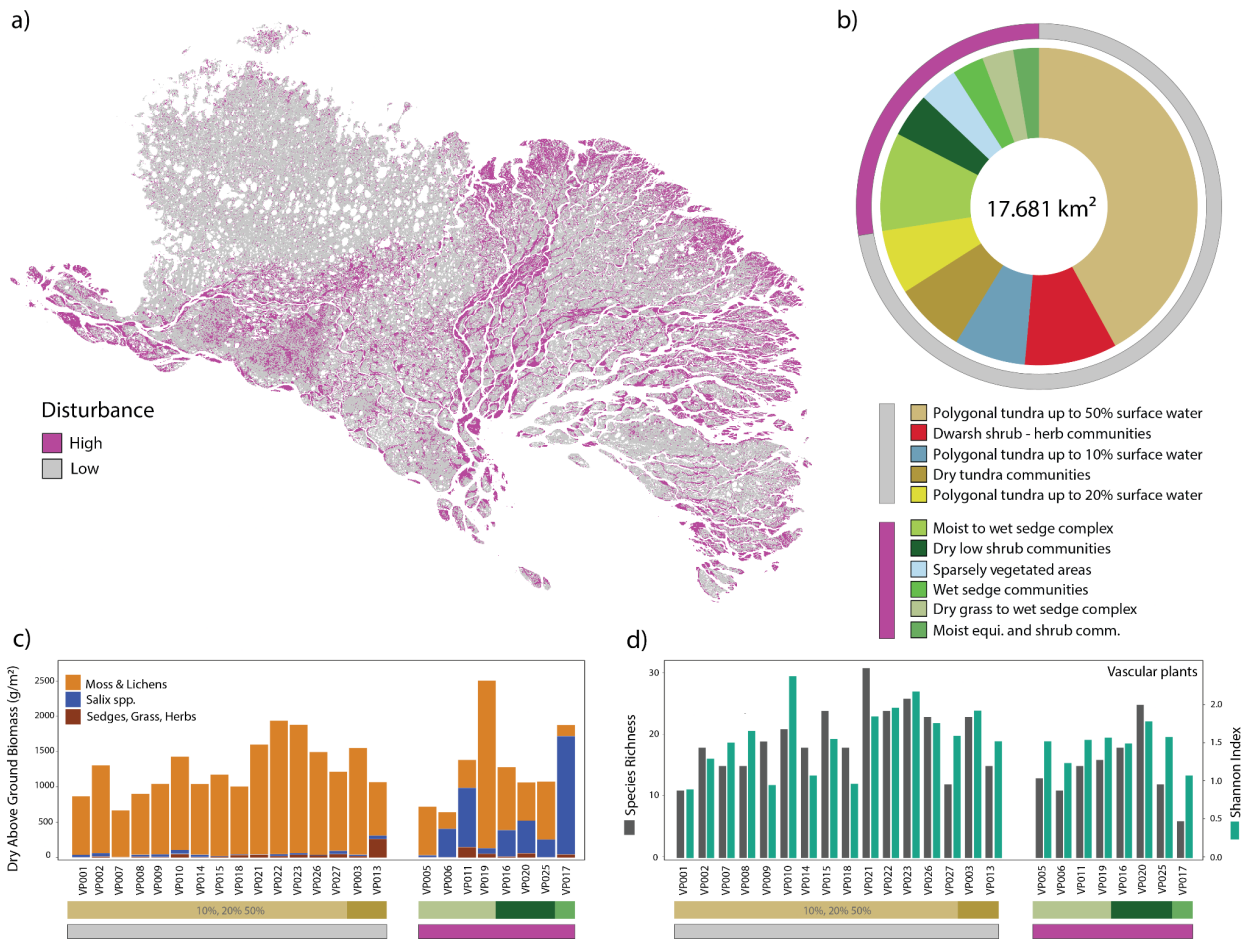1036   habitat classes.

Figure 6: Habitat linked disturbance regimes across the Lena Delta. The map (a) includes all vegetated areas (excluding water and sand). The pie chart (b) shows the contribution of vegetated classes across the Lena Delta grouped by high and low disturbance regimes. The bottom panels show c) the measured dry above ground biomass (Dataset 2) and d) the species richness and Shannon index (from Dataset 1) of the vegetation plots for different habitat classes and disturbance regimes.

Tables

Table 1: Habitat classes, descriptions as well as methods used to characterize the distinct habitats. In-situ vegetation plot numbers correspond to the vegetation plots of Dataset 1 and 2 (see also Table S1, S2, S3).

Habitat types	Description	Method
Moist *Equisetum* and shrubs	*Equisetum* and shrub communities form a early-to-middle successional stage growing on the active floodplain. Low moss contribution	In-situ vegetation plot (VP17); extended to representative larger polygon shape files using field knowledge.
Dry shrub communities	Patch forming shrub communities dominated by dwarf willow (*Salix*) thickets, frequently occurring on dry elevated areas on floodplains and stream floodplains and in topographically sheltered areas below basin and valley rims. Low moss contribution	In-situ vegetation plots (VP04, VP16); extended to representative larger polygon shape files using field knowledge.

Polygonal tundra complex
 	
up to
   -    10%
   -    20%
   -    50% surface water
 	
(3 distinct classes)
	Mature-state plant communities dominated by sedge, moss and herb species. Sparse vascular plant coverage (dwarf willows, dwarf birches) on thick continuous moss cover. Occurring on the plateaus of the ice-rich holocene and pleistocene terraces, and at the bottom of alases. Intersected by intra- and interpolygonal ponds resulting in up to 10%, 20%, 50% surface water contribution.	In-situ vegetation plots (VP01, VP02, VP07, VP08, VP14, VP15, VP18, VP21, VP22, VP23, VP26, VP27); extended to representative larger polygon shape files using field knowledge. The different surface water contributions were defined based on the result from unsupervised classification.

41

Dry grass to wet sedge communities	These early-to-middle successional plant communities cover unstable valley slopes and a young drained lake basin, they are mostly composed of sedges and grasses, but also willows (*Salix)* are part of this habitat.	In-situ vegetation plots (VP05, VP06, VP11, VP19, VP20); extended to representative larger polygon shape files using field knowledge.
Dry tundra communities	The mature-state dry tundra communities represent the zonal tundra type, one subclass is dominated by tussock forming *Eriophorum* and the other by less tussock forming dry-herb communities, dominated by *Dryas*. Occurring on well-drained slopes of valleys and alases, and other well-drained areas on the terraces. High moss contribution	In-situ vegetation plots (VP03, VP13) extended to representative, larger polygon shape files using field knowledge (including 'dry tundra communities type tussock' and 'dry tundra communities').
Moist to wet sedge communities	These mid to advanced successional plant communities occur on moist to water-logged soils characteristically mostly in topographic depressions on the floodplains, in valleys and alases. They constitute the rims of the wetland areas on the floodplains in more dynamic parts the moss ground cover is missing.	Polygon shape files derived from high resolution satellite image and ESRI GE with regional expert knowledge. No vegetation plots (too wet).
Wet sedge communities	These mid to advanced successional plant communities occur at permanently wet sites with stagnant water in the topographic depressions and are typical for wetland areas on the floodplains. In more dynamic parts the moss ground cover is missing.	Polygon shape files derived from high resolution satellite image and ESRI GE with regional expert knowledge. No vegetation plots (too wet).

Sparsely vegetated areas	These early successional plant communities are characterized by low vegetation establishment and coverage. No to low moss contribution	Defined based on the result from unsupervised classification, polygon shape files. No vegetation plots.
Barren/Sand	Representing the wide-open sand flats of the floodplain and barren ground on valley slopes or along cliffs. In a few cases, this class represents vegetation-free bedrock outcrops.	Threshold using high reflectance in S2-band 2 blue.
Water	Represents all surface water bodies in the delta: the Lena River with river branches, streams, lakes and large ponds.	Threshold using low reflectance in S2-band 8 NIR.

1050

1051 Table 2: Habitat class and description of disturbance regimes and the component stand
1052 structure in form of contributions of vascular plants, and moss to total biomass. * (Driscoll and
1053 Hauer, 2019; Stanford et al., 2005), ** (Lorang and Hauer, 2006).

Habitat class	Disturbance regime	Stand structure
Moist *Equisetum* and shrubs	**High; regular (annually), predicted** - spring floodings, - shifting habitat * - advanced-stage regeneration **	high vascular plant growth, low abundance of moss & lichens.
Dry shrub communities	**High; mixed disturbance types**: -regular spring floodings -rapid thaw processes (permafrost degradation) - shifting habitat - advanced-stage regeneration	high vascular plant growth, low abundance of moss.
Polygonal tundra complex	**Low; mixed disturbance types** - low for most of the habitat, except for actively eroding shores of ponds and channels - mature-state plant community	low vascular plant growth, high abundance of moss.
Dry grass to wet sedge communities	**High; mixed disturbance types**: - regular spring floodings - rapid thaw processes (permafrost degradation) - shifting habitat	high vascular plant biomass, low abundance of moss.

44

	- advanced-stage regeneration	
Dry tundra communities	**Low; mixed disturbance types** - low for most of the habitat - mature-state plant community	low vascular plant biomass high abundance of moss.
Moist to wet sedge communities	**High; mixed disturbance types**: - regular spring floodings - rapid thaw processes (permafrost degradation) - shifting habitat - mid to advanced-stage regeneration	high vascular plant biomass Almost impossible to measure in-situ biomass (wet conditions and difficult access).
Wet sedge communities	**High; mixed disturbance types**: - regular spring floodings - rapid thaw processes (permafrost degradation) - shifting habitat - mid to advanced-stage regeneration	high vascular plant biomass. Almost impossible to measure in-situ biomass (wet conditions and difficult access).
Dwarf shrub herb communities	**Low; mixed disturbance types** - low for most of the habitat - mature-state plant community	low vascular plant biomass, high abundance of moss.

Sparsely vegetated areas	**Very high; mixed disturbance types** - regular spring floodings - rapid thaw processes (permafrost degradation) - shifting habitat - early-stage regeneration	lowest vascular plant biomass, no moss.
Sand banks/barren	**Very high: mixed disturbance types** - regular spring floodings - rapid thaw processes (permafrost degradation) - shifting habitat - no regeneration	Barren, constant shifting of sediments and movement of soils.

1054